國立臺灣大學生命科學院植物科學研究所

碩士論文

Institute of Plant Biology, College of Life Science
National Taiwan University
Master Thesis

阿拉伯芥熱休克因子結合蛋白在熱逆境反應及

生長發育時期之功能性研究

Functional Study of Heat Shock Factor Binding Protein (HSBP) in

Heat Stress Response and Development Stages of Arabidopsis

李怡潔

Yi-Jie Li

指導教授：靳宗洛 教授

Advisor: Tsung-Luo Jinn, Ph. D

中華民國 106 年 10 月

October, 2017

致謝

在植科所不知不覺也過了 3 年的時間了，能夠順利完成碩士論文，首先要感謝的就是 R913 實驗室的大家長靳宗洛老師，謝謝老師提供完善的環境及資源並適時地提供寶貴的建議讓我的論文更加的充實完整，也感謝鄭貽生老師、張英峯老師、葉靖輝老師以及吳慧珍老師擔任我的口試委員，以及其餘植科所老師平時給的建言也給予了我許多專業上的建議。

對於實驗室裡一起打拼的夥伴們，感謝你們陪伴我度過了這段充滿歡樂以及淚水的歲月。謝謝勤政學長為我的研究題目打下良好的基礎，雅貞學姊總是和我們打成一片卻不厭其煩的指導我們實驗的進行，佩君你像是實驗室的歡笑來源，有你在的地方總是充滿著笑聲，對於共同打拼 3 年的胤達和敬智，感謝彼此之間的互相幫忙和激勵，希望你們替代役生涯順利，謝謝 Lynne 為實驗室帶來了不同的文化氣息，也常常幫助大家有關英文方面的問題，更讓大家養成運動的好習慣，希望伊卉、期敏、中仁和俊夆可以成為實驗室未來的支柱好好的帶領心盈、適宇以及 Hary。最後，我要感謝我的家人在這 3 年的期間，給予了我最有力的後盾。

<div align="right">2017,10 怡潔</div>

Table of Contents

ABSTRACT

Arabidopsis heat shock factor binding protein (HSBP) has been reported as a negative

regulator required for the attenuation of the heat shock response (HSR) by binding to

the heptad repeat regions of HSF through its coiled-coil domain. In addition, three

distinct phenotypes were observed in the HSBP-mutant plants, including early flowering,

shorten silique length and one-third ratio of seed abortion. To decipher the molecular

mechanisms behind these phenotypes and the functions of HSBP in developmental

stages, I identified the interacting proteins of the HSBP through immunoprecipitation

assay followed by the LC-MS/MS analysis. Cytoskeleton-associated proteins COP1

interactive protein1 (CIP1) and kinesin like protein for actin based chloroplast movement

1/2 (KAC1/2), as well as the ER-localized proteins, Maigo2 (MAG2) and MAG2-interactive

protein1/2/3 (MIP1/2/3) were identified and confirmed as HSBP interacting proteins.

HSBP along with CIP1 has effects on Constitutive photomorphogenic 1 (COP1) to

participate the downstream flowering-time genes expression and photomorphogenesis

control. The unprocessed seed storage protein precursors were detected in *hsbp* seeds

with mis-shapen phenotype, indicating the possible role of HSBP in the intracellular

protein trafficking and the seed maturation. The interaction between HSBP and KAC1/2

provides the insight into chloroplast cp-actin movement regulation. Since the coiled-coil domain is the only functional domain in HSBP, it is very important for its structure formation as well as the biological functions. The Arabidopsis HSBP-T17C and -R48K mutations cause the alteration of oligomerization status whereas the S35A variant restrains HSBP from entering into the nucleus. The I42K/M45K and I49K/L52K variants cause effects on heat stress tolerance ability. Together, we concluded that the mechanisms of HSBP versatile functions in response to heat stress and in the development stages in *Arabidopsis thaliana*.

Keywords: HSBP, interacting proteins, photomorphogenesis, seed storage proteins, coiled-coil domain, oligomerization status.

摘要

在前人研究中，阿拉伯芥熱休克因子結合蛋白(Heat Shock Factor Binding Protein,

HSBP)已被證明透過利用自身的卷曲螺旋結構和熱休克因子(Heat Shock Factor, HSF)

上的七胜肽重複區結合以達到在熱休克反應後期擔任負調控者的角色。在 HSBP 缺

失的阿拉伯芥突變株中，我們觀察到了三個明顯的表現型缺陷，包括開花期的提

早、果莢短小以及種子缺失三分之一的現象。為了瞭解這些表現型發生背後的分子

機制，本篇研究中篩選並確認了 HSBP 的交互作用蛋白，包括光型態發育持續表現

蛋白的交互作用蛋白一號(CIP1)、葉綠體移動類驅動蛋白一號及二號(KAC1/2)、種子

儲存蛋白(MAG2)以及其三個共同作用蛋白(MIP1, 2 以及 3)。HSBP 和 CIP1 共同作

用，參與光型態發育持續表現蛋白(COP1)影響開花時間以及光型態發育的調控。在

HSBP 突變株中偵測到不正常種子儲存蛋白的前驅物存在，暗示其在種子發育中可

能扮演的角色。由於卷曲螺旋區域是 HSBP 的唯一功能性區域，推測其對結構的穩

定性及功能是非常重要的。HSBP 卷曲螺旋區域 T17C 以及 R48K 突變造成了聚合狀

態的改變，而 S35A 突變則是會限制 HSBP 在細胞質而無法進入到細胞核中，

I42K/M45K 以及 I49K/L52K 突變株則是會對植株的耐熱性造成影響，結果確認卷曲

螺旋對於 HSBP 結構以及生理功能具重要性。總體而言，本篇研究探究了 HSBP 在

阿拉伯芥生長發育階段以及對抗熱逆境時所扮演的角色。

關鍵字：熱休克因子結合蛋白、卷曲螺旋、交互作用蛋白質、光型態發育、種子發

育及儲存蛋白質

ABBREVIATIONS

HSBP: Heat Shock Factor Binding Protein

HSR: Heat Shock Response

HSF: Heat Shock Factor

HSE: Heat Shock Element

CIP1: COP1-interactive Protein 1

COP1: CONSTITUTIVE PHOTOMORPHOGENETIC 1

KAC1/2: Kinesin-like Protein for Actin-based Chloroplast Movement 1/2

MAG2: Maigo 2

AtZW10: Putative Centromere/Kinetochore Protein ZW10

Sec39: Secretory Pathway 39

CO: CONSTANS

FT: FLOWERING LOCUS T

HR: Heptad Repeat

INTRODUCTION

Heat Shock Response and Thermotolerance

One of the major factors representing a significant barrier to life is the heat stress.

It takes only mild temperature increase to create stresses in living cells, such as protein

unfolding, entanglement and unspecific aggregation, which can all lead to abnormal

physiological functions. These detrimental protein accumulations are considered as

partial signals to initiate the heat shock response (HSR) as a counter measure (Kotak et

al., 2007; Richter et al., 2010; Bokszczanin and Fragkostefanakis, 2013). Plants as

immobilized organism are routinely challenged by surrounding abiotic and biotic

stresses especially the heat stress and have developed a wide range of heat shock

responses referred as "thermotolerance" to cope with heat stress.

To live under temperatures higher than optimal conditions, plants like other

organisms exhibit basal thermotolerance (BT) due to their inherent ability, but plants are

also equipped with the ability to acquire tolerance to lethal heat shock (LHS) called

acquired thermotolerance (AT) (Ahuja et al., 2010; Bokszczanin and Fragkostefanakis,

2013). While land plants constitutively carry out basal thermotolerance (BT) to

withstand the inevitable weather changes, it is also necessary for them to conditionally

11

expressed short-termed AT at the cellular and molecular levels to cope with acute

temperature changes. The acquisition of thermotolerance is an autonomous cellular

phenomenon and normally results from prior exposure to a conditioning moderate level

of HS pretreatment. This priming pretreatment provides plants with resistance against

the LHS (Ahuja et al., 2010; Qin et al., 2011; Yeh et al., 2012).

Heat Shock Proteins and Heat Shock Factors

Heat shock proteins (HSPs) are groups of proteins induced by stresses. Functionally,

these stresses inducible proteins can be classified into seven classes. The first and the

most dominant one is commonly referred as "molecular chaperones", the members of

second class are involved in proteolytic system which clear irreversible misfolded or

aggregated proteins from cell. The third class is engaged in repairing nucleic acids that

are damaged by heat stress. The fourth class of HSP is composed of metabolic enzymes

and the fifth class includes regulatory proteins, for example, kinase enzymes are needed

to trigger further downstream stress responses or inhibit expressive gene cascades. The

sixth class comprises proteins maintain the cellular structures such as the cytoskeleton.

At last, the seventh class of HSP contains trafficking, detoxifying, and membrane-

bounding proteins (Richter et al., 2010).

The predominant class of HSP, the molecular chaperones, consists of five major and highly conserved families HSP100s, HSP90s, HSP70s, HSP60s, and small heat shock proteins (sHSPs). Interestingly, under normal growing condition, chaperones assistant the *de novo* protein folding and the refolding of polypeptides. One of the most common chaperone is the HSP70 protein, which is found in the cytosol and organelles, such as the ER, mitochondria and chloroplasts. HSP70 facilitates proper folding of newly synthesized proteins while the activity of HSP70 is largely regulated by its cofactors. The main class of HSP70 cofactor is HSP40/ J-domain-containing proteins, which interact with the ATPase domain of HSP70 and stimulate the hydrolysis of bound ATP (Mayer and Bukau, 2005; Sun and MacRae, 2005). High concentration of HSP90 exists in the cytosol area of both prokaryote and eukaryote cells and is upregulated under stresses. The differences between HSP70 and HSP90 are that HSP90 does not have as many cofactors as HSP70 does and it mainly interacts with *de novo* proteins instead of misfolded proteins. Regarding to the theme of heat shock response, sHSPs represent a variation of protecting proteins from irreversible aggregation or degradation by cooperating with chaperones. Functionally, sHSPs are ATP-independent chaperones that can assemble

13

into polymer structures and interact with target proteins to prevent their aggregation upon stress-induced unfolding (Sun and MacRae, 2005).

Among the heat stress regulatory network, heat shock transcription factors (HSFs) convert stress signals to stress responsive genes by recognizing the palindromic binding motifs, the so-called heat stress elements (HSEs; 5'-nGAAnnTTCn-3') conserved in the promoter regions of heat stress inducible genes (von Koskull-Doring et al., 2007; Guo et al., 2016). In *Arabidopsis thaliana*, there are a total of 21 HSFs categorized into 3 classes (A, B, and C) based on structural characteristics and phylogenetic relationships.

The highly structured and conserved DNA-binding domain (DBD) locates at the N-terminus of all three classes of HSFs. The two arrays of hydrophobic heptad repeat oligomerization domain (HR-A/B) locates adjacent to DBD connected by flexible linker, which consists of 9 to 39 amino acids for class A, 50 to 78 amino acids for class B and 14 to 49 amino acids for class C HSFs. The HR-A/B region of class B HSFs are similar to all non-plant HSFs, whereas all class A and class C HSFs have an extended HR-A/B region due to the insertion of 21 (class A) and 7 (class C) amino acid residues between the HR-A and -B regions. Class B and C HSFs lack the activator motif AHA that is necessary for the transcriptional activity of class A HSFs and are therefore considered as inhibitors

14

(Nover et al., 2001; von Koskull-Doring et al., 2007; Mittler et al., 2012; Guo et al., 2016).

A tremendous importance for the HSR is attributed to the observed HSP-HSF complexes.

HSF-chaperone interactions are thought to regulate HSR mechanisms by sensing the

demand of chaperones under continuously changing HS conditions

Heat Shock Factor Binding Protein

Heat shock factor binding protein (HSBP) is a highly conserved small heat-

responsive protein among eukaryotic species except in yeast. The first HSBP was

identified in humans (*Homo sapiens*) named as HSBP1. Previous studies about HSBP1

indicated that it is a nuclear-localized protein and interacts with oligomerization motif of

HSF1 by the coiled-coil domain (Satyal et al., 1998; Tai et al., 2002). The following

research conducted on *Caenorhabditis elegans* also showed the same results suggested

that the significance of coiled-coil domain on HSBP1 structure and the physiological

functions (Satyal et al., 1998).

The crystallization structure study revealed that a continuous, long-helix

conformation of HSBP1 which assembled into a coiled-coil three-helix bundle and

subsequently into an elongated, N-terminus to N-terminus symmetrical hexamer (Tai et

al., 2002; Liu et al., 2009). Interestingly, further researches on *Plasmodium falciparum* and human HSBP structure compositions stated that HSBP1 exists as mixture of trimer and hexamer by the native gel examination, SDS-PAGE analysis, and size exclusion chromatography. Therefore, a trimer-hexamer equilibrium model was proposed (Tai et al., 2002; Liu et al., 2009; Sayeed et al., 2014).

In planta, HSBP homologues in maize (*Zea mays*), rice (*Oryza sativa*), and Arabidopsis are also studied. There are two HSBP paralogs in maize, *EMPTY PERICARP 2* (*EMP2*; i.e., *HSBP1*) and *HSBP2*. EMP2 encodes the first described HSBP-like protein in plants. The *emp2* defective-kernel mutation of maize is a recessive lethal mutation indicating that EMP2 is necessary for the proper embryogenesis, whereas accumulation of HSBP2 is induced in seedlings following HS similar to HSBP1 affecting embryo development in humans (Fu et al., 2002; Fu and Scanlon, 2004; Fu et al., 2006; Eroglu et al., 2014). Besides, site-specific mutagenesis of HSBP2 within the hydrophobic region also implied that coiled-coil domain is required for the HSBP2-HSFs interaction. In addition, two putative HSBP homologues were reported in rice (*Oryza sativa* L. Subsp. *Japonica*), *OsHSBP1* and *OsHSBP2*. Both genes expressed ubiquitously in all tissues under normal growth condition and were significantly induced during the HSR and the

following recovery phase. Other than the activity in HSR, the gene knock-down plants showed arrested developments of the ovaries and seed abortion phenotype suggested that cytoplasm-nuclear localized *Os*HSBP1 and *Os*HSBP2 were also involved in the regulation of embryogenesis and seed development after fertilization (Rana et al., 2012).

Notably, only one homolog of HSBP in Arabidopsis is identified as AtHSBP. *AtHSBP* (At4g15802), which has five exons and four introns that encodes 86 amino acid residues with predicted molecular mass of 9.35 kDa and p*I* 4.11. It is also ubiquitously expressed in all tissues but have especially higher expression at siliques. The cytoplasm-nuclear localized AtHSBP primarily distributes in cytoplasm and translocated into nucleus while exposed to heat stress to attenuate HSR during the recovery phase.

AtHSBP have already been proved to interact with several HSFs. In the loss-of-function *hsbp* mutant line, three distinct phenotypes were observed, including early flowering, shortened silique, and 30% seed abortion. Because AtHSBP only have one functional domain, coiled-coil domain, it is reasonable to assume that AtHSBP mediates HSR and physiological functions through coiled-coil domain interactions with HSFs and other potential interacting proteins (Hsu and Jinn, 2010; Hsu et al., 2010)

The Coiled-Coil Domain

Protein oligomerization is one of the fundamental strategy to mediate various

cellular mechanisms. The basic and common oligomerization motif is the coiled-coil

motif. The coiled-coil structural motif comprises two or more right-handed helices

tangled around each other with a small, left-handed superhelical twist and each helix

has seven repeats of proteins (*a, b, c, d, e, f,* and *g*) (Mason and Arndt, 2004; Truebestein

and Leonard, 2016). In this periodic repeat model, the "*a*" and "*d*" residues are typically

hydrophobic nonpolar found occupying the interhelical interface. Studies showed that

the shapes and types of hydrophobic residues stabilize the oligomerization helices

through hydrophobic and van der Waals interactions. The "*e*" and "*g*" are charged and

polar residues giving specificity between the two helices through electrostatic

interactions (Mason and Arndt, 2004; Ciani et al., 2010).

Prominent examples of coiled-coil motif containing proteins include desmin and

keratin forming the skeleton of intermediate filaments. In the case of human HSBP1

(hHSBP1), it is known that HSBP1 interacts with HSF1 through binding to the HSF1 HR-

A/B region by coiled-coil domain and hHSBP1 is the first protein that has been described

that is composed solely of a coiled-coil domain. This suggested the important and

irreplaceable function of HSBP. The crystal structure of hHSBP1 indicated that each

single-helix molecule forms parallel coiled-coil homo-trimers with its own symmetry

mates; furthermore, the two hHSBP1 trimers assembled into hexamer structure in a

head-to-head fashion (Tai et al., 2002; Liu et al., 2009; Ciani et al., 2010).

Interacting Proteins of Heat Shock Factor Binding Protein

There were three groups of HSBP-interacting proteins been identified according to

previous studies (Liu and Jinn, 2014). First, a group of cytoskeleton-associated proteins

were identified, including COP1-interactive protein1 (CIP1, At5g41790), CIP1 like (CIP1L,

At1g64330), and Kinesin-like protein for actin-based chloroplast movement 1/2 (KAC1/2,

At5g10470 and At5g65460).

CIP1 was previously proved to be involved in the nucleocytoplasmic partition of

COP1 by coiled-coil domain formation. Despite its interactive protein COP1 was a key

repressor of photomorphogenesis, CIP1 was reported not to be regulated by light signals.

CIP1 mediated the light control of nuclear COP1 activity by sequestering COP1 in the

cytoplasm under the light condition, thereby impending its nuclear import in Arabidopsis

(Matsui et al., 1995; Osterlund et al., 1999; Jang et al., 2015). Recent studies also

19

revealed that CIP1 was a positive regulator of abscisic acid (ABA) response and could be

activated by osmotic stress (Ren et al., 2016).

Organelles move within cells dynamically and localized to appropriate positions to

accomplish their functions; therefore, it is pivotal for organelles to move efficiently to

function properly. The chloroplast photo-relocation movement is mediated by short

actin filament regulation on chloroplasts (i.e., cp-actin filaments). Chloroplasts have to

attach to the plasma membrane to relocate and this anchoring mechanism is also tightly

regulated by actin filaments (Suetsugu and Wada, 2007; Suetsugu et al., 2012). Previous

studies reported that kinesin-like proteins, KAC1 and KAC2 were essential for

chloroplasts movement (Suetsugu and Wada, 2007). KAC1 belongs to the kinesin-14

family and has a homolog gene *KAC2* in Arabidopsis. The chloroplasts movement in *kac1*

mutant was severely damaged then resulted in slow avoidance movement and in the

kac1kac2 double mutant, the chloroplasts photo-relocation is completely lacked;

therefore, the chloroplasts were detached from the plasma membrane. This suggests

that KAC1 and KAC2 are important regulators for the actin-mediated chloroplast

movement. By the COILS program prediction, the KAC proteins contain coiled-coil

domains at the N-terminal and the middle regions of the proteins (Suetsugu and Wada,

2007; Suetsugu et al., 2012; Shen et al., 2015).

Other than the cytoskeleton-associated proteins, a group of endoplasmic-reticulum (ER) protein was also identified as HSBP-interacting proteins, including MAG2 (Maigo2, At3g47700), along with three its interacting proteins MIP1 (MAG2-interacting protein1, putative centromere/kinetochore protein (ZW10), At2g32900), MIP2 (MAG2-interacting protein 2, putative Sec39 domain-containing protein, At5g24350), and MIP3 (MAG2-interacting protein 3, putative Sec1-like domain-containing protein, At2g42700) (Shimada et al., 2003; Li et al., 2013; Mylne et al., 2014).

Intracellular trafficking between cellular organelles is very important for the fundamental cellular activities. Multisubnuit tethering complexes (MTCs) are reported to be essential for adequate intracellular trafficking and MTCs function in the initial interactions of transport vesicles with their target membrane prior to membrane fusion. From previous studies, multiple MTCs and related soluble N-ethylmaleimide-sensitive factor attachment protein receptors (SNAREs) were discovered. The first one is the Dsl1 tethering complex, consisted of three core subunits of Dsl1p, Sec39p/Dsl3p, and Tip20P, founded in *Saccharomyces cerevisiae* (Tagaya et al., 2014). The Dsl1 complex binds to SNARE protein acceptor complex and transport vesicles retrogradely from the Golgi

complex to ER. The function of Dsl1 complex was considered as conserved and several

equivalent complexes were also discovered in higher eukaryotic organisms (Shimada et

al., 2003; Li et al., 2006; Li et al., 2013; Zhao et al., 2013).

The NRZ (NAG: RINT1: ZW10) tethering complex (mammalian Dsl1 complex) was

identified in human, which Zesto-White 10 (ZW10, homolog of Dsl1p) protein interacted

with NAG and RINT1 (Tagaya et al., 2014), while the MAG2 complex was later discovered

in Arabidopsis. The MAG2 (Maigo2) interacted with ZW10 to form the potential MTC and

to facilitate the Golgi-to-ER trafficking. The MAG2 complex contained MAG2 and other

two core subunits, including MIP1, the 83.9 kDa protein with a conserved ZW10 domain

and MIP2, the 266.8 kDa protein that contains a Sec39 domain. Previous studies have

shown that MAG2 is responsible for the protein transportation between the ER

membrane and the Golgi apparatus. It was also revealed that in *mag2* mutant line, the

abnormal seed storage protein accumulation was observed in Arabidopsis dry seeds. The

aberrant aggregation was identified as the precursors of seed storage proteins 2S

albumin (p2S) and 12S globulin (p12S) (Li et al., 2006; Mylne et al., 2014). The mutant

lines *mip1* and *mip2* also showed the similar effects on precursor proteins accumulation

(Li et al., 2006; Li et al., 2013).

Gene Regulations of Flowering Pathway in Arabidopsis

The transition from vegetative phase to reproductive phase is one of the key developmental stage that is under sophisticated regulations. During this floral induction process, the shoot apical meristem starts to generate flowers instead of leaves. The timing of the transition is coordinated with environmental and physiological signals to ensure the maximum reproduction success and seed production. In Arabidopsis, the flowering regulation can be roughly categorized into six major pathways, the photoperiod and vernalization pathways control flowering in response to seasonal changes in day length and temperature; the ambient temperature pathway responds to daily growth temperatures; and the age, autonomous, and gibberellin pathways act more independently of environmental stimuli (Amasino and Michaels, 2010; Fornara et al., 2010). These pathways together regulate a small number of floral integrator genes which govern flowering time by incorporating multiple signals. These integrator genes include *FLOWERING LOCUS T* (*FT*) and S*UPPRESSOR OF OVEREXPRESSION OF CONSTANS 1* (*SOC1*), which both rapidly promote floral development.

The vernalization pathway stimulates flowering by silencing *FLOWERING LOCUS C* (*FLC*), a MADS-box transcription factor gene that acts as a strong repressor in the

23

flowering signal pathway, in response to lengthened exposure to low temperature. The

maintenance to *FLC* repression after plants returned to warmer temperature requires

the histone modification at the chromatin locus of *FLC*. Flowering of Arabidopsis is also

regulated by seasonal rhythm, which would be promoted in the summer long days and

repressed in winter short days. During long days, light boosts the interaction between

GIGANTEA (GI) and a family of F-box ubiquitin ligases. This can stabilize the F-box

proteins, allowing them to promote the degradation of a set of repressors, including

CONSTANS (CO). At the posttranscriptional level, CO is degraded by the ubiquitin ligase

CONSTITUTIVE PHOTOMORPHOGENIC 1 (COP1) in the dark and promoted by

photoreceptor phytochrome B (PHYB) in daylight (Amasino and Michaels, 2010; Fornara

et al., 2010).

The circadian clock regulation comprises three interlocked feedback loops. The

central loop includes transcription factors CIRCADIAN CLOCK ASSOCIATED1 (CCA1) and

LATE ELONGATED HYPOCOTYL (LHY), which repress the transcription of TIMING OF CAB1

(TOC1). Arabidopsis flowers earlier when grown at higher temperatures, such as 23°C,

than at lower temperatures, such as 16°C and the MADS box transcription factor SHORT

VEG-ETATIVE PHASE (SVP) appears to play a crucial role in this pathway (Amasino and

Michaels, 2010; Fornara et al., 2010; Golembeski and Imaizumi, 2015).
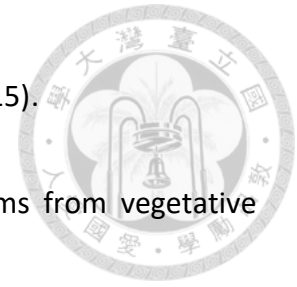
During floral induction, the shoot apical meristem transforms from vegetative meristem into inflorescence meristem to grow flowers. The floral gene integrator SOC is activated by gibberellin (GA) and aging while repressed by vernalization and ambient temperature pathways by the inhibition of FLC and SVP. SOC also requires FT, which migrates from leaves to meristem in the long days to initiate flower development by interacting transcription factor FD and promoting MADS-box factor AP1 (Baurle and Dean, 2006; Fornara et al., 2010).

Seed Storage Proteins of Arabidopsis

Plant storage proteins comprise two classes, the seed storage proteins (SSPs) and vegetative storage proteins (VSPs). SSPs have high accumulation level at the late stages of seed development, whereas VSPs accumulate at the vegetative tissues. When seed germination occurs, the SSPs are degraded as the nutritional source. The major SSPs of Arabidopsis include 12S globulins and 2S albumins, based on their solubility to water and salt solution. Both 12S globulins and 2S albumins are first synthesize as precursors in the protein bodies and furthermore processed into mature form proteins (Fujiwara

et al., 2002; Mylne et al., 2014).

Like most of other plants, Arabidopsis SSPs are encoded by a small group of family

genes. Five isoforms of genes encoding 2S albumin referred to as *At2S1* to *At2S5* while

12S globulins of Arabidopsis were encoded by *CRA1*, *CRB,* and *CRC* gene. Other than the

12S and 2S storage proteins, 7S globulin is also one of the major SSPs. However,

Arabidopsis does not contain detectable 7S globulin (Fujiwara et al., 2002; Mylne et al.,

2014).

Motivation and Objectives

Previous studies on HSBP revealed that HSBP translocated into the nucleus and

functioned as a negative regulator during the attenuation stage of the HSR. Three

apparent physiological defects were observed in the *hsbp* mutant besides the expected

prolonged and boosted HSR, including early flowering, shorten silique length and the

one third ratio of seed abortion. This indicates that HSBP has more potential functions

than just a negative regulator in the HSR.

The first objective of this research is to discover the role of HBSP in the growth and

development of Arabidopsis by screening for HSBP interacting proteins. Then the

relations between HSBP and the selected interacting proteins will be determined to

decipher the function of HSBP in the growth and development stages.
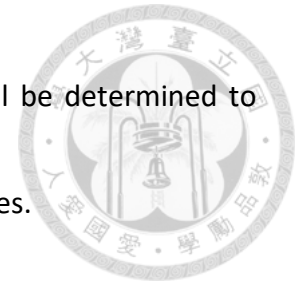
HSBP harbors heptad repeats in the central region, which creates the coiled-coil

domain. The coiled-coil domain is the only functional domain of HSBP which provides

the stability of both biological function and structure. Previous studies on human

revealed the crystal structure of HSBP1 as two homo-trimers formed into the hexamer

structural form, and our studies on Arabidopsis showed that the point mutation S35A at

coiled-coil domain region prevented HSBP from entering into the nucleus and resulted

in the phenotype changes. The second objective is to create series of point mutations

within the heptad region of Arabidopsis HSBP and evaluate the structural deformations

as well as the effects on the physiological alterations.

27

MATERIALS AND METHODS

Plant Materials and Growth Conditions

Arabidopsis thaliana (Columbia) was used as the wild type (WT). The *HSBP* (At4g15802) T-DNA insertion mutant *hsbp* (SALK_081104; *hsbp-1*) was previously characterized (Hsu et al., 2010). The CIP1 (At5g41790) and MAG2 (At3g47700) T-DNA insertion mutants *cip1* (SAIL_841_A08.V1) and *mag2* (SALK_037370) were obtained from the Arabidopsis Biological Resource Center (ABRC; Ohio State University). The mutant lines *kac1-2, kac2-2,* and *kac1-2 kac2-2* were provided by Dr. Masamitsu Wada of Kyushu University. The *CaMV 35S*-driven *HSBP-3xFLAG* and *HSBP-GFP* lines were as described (Hsu and Jinn, 2010; Hsu et al., 2010).

The upstream 1.5 kb potential *HSBP* promoter region along with the *HSBP* open reading frame (ORF) harboring *Bam*HI and *Nco*I sites was PCR-amplified and cloned to the pCHF3-3xFLAG, then the whole 3-kb *proHSBP::HSBP-3xFLAG* plus the following RbcS terminator was subcloned to the pCAMBIA3300 construct via the *Pst*I site to generate the transgene of native-HSBP promoter driven *HSBP-3xFLAG* expression. The coding regions of three representative interacting proteins, *CIP1, MAG2,* and *KAC1* were cloned to pCR™/GW/TOPO® then subcloned to the *p*2FGW7 to generate the *35S::GFP-CIP1, -*

28

MAG2, and *-KAC1* constructs. The 1.5 kb potential promoter region of HSBP was cloned

to pCAMBIA1391z via *Bam*HI and *Eco*RI sites to generate the *proHSBP::GUS* construct.

Agrobacterium tumefaciens-mediated genetic transformation of Arabidopsis

involved the floral-dip method (Clough and Bent, 1998). Plants were grown in growth

chambers at 22°C under 16 h light/8 h dark at 60 to 100 µmol m^{-2} s^{-1} and screened with

use of 0.4% (v/v) BASTA herbicide (Farnam Companies).

DNA/RNA Extraction, RT-PCR and Quantitative PCR (qPCR)

For plant tissue genomic DNA extraction, tissues were frozen by liquid N$_2$ and

grounded then mixed with DNA extraction buffer (7 M Urea, 0.3 M NaCl, 50 mM Tris-HCl,

pH8.0, 20 mM EDTA, pH 8.0; 1% N-laurylsarcosine) and phenol: chloroform: isoamyl

alcohol (25: 24: 1). After centrifugation, upper water phase layer was added with equal

volume of chloroform then subjected to another centrifugation. Upper water phase

layer was transferred to new Eppendorf and mixed with isopropanol (IPA) to precipitate

DNA. Supernatant was discarded after centrifugation and pellet was washed with 75%

ethanol for at least two times. Air dried DNA pellet was resolved in ddH$_2$O.

For plant tissue RNA extraction, tissues were frozen by liquid N$_2$, grounded then

29

mixed with TRIzol® reagent (Invitrogen) and chloroform, the upper water phase was

separated after centrifugation. IPA was then added and let stand at 4°C for at least an

hour to precipitate RNA. After centrifugation, supernatant was removed and pellet was

washed with 75% ethanol for three times then air-dried in damp-proof cabinet. Dried

RNA pellet was then dissolved in DEPC-H_2O and heated to 55°C. To remove the extra

DNA in the RNA sample, TURBO™ DNase buffer and DNase enzyme was added into

sample in order and react under 37°C water bath for 30 minutes and added with DNase

inactivation agent to terminate the reaction. Reverse transcription kit (Invitrogen) was

used for cDNA synthesis. The quantitative PCR (qPCR) is conducted by ABI 7500 Real-

Time PCR machine (Applied Biosystem).

ß-Glucuronidase (GUS) Activity Assay and Cleared Tissue for Observation

Collected samples were first submerged in the fix solution (20 mL 0.1M NaPO4,

pH7.0; 200 μL formaldehyde; 200 μL Triton X-100; 200 μL *ß*-mercaptoethanol) and

vacuumed in the sealed tank for 5 min. Samples were then washed with 0.1 M $NaPO_4$

buffer for 2 times and stained with the staining buffer (1 M Na_2HPO_4, 1 M NaH_2PO_4, 0.05

M $K_3[Fe(CN)_6]$, Triton X-100, 0.05 M $K_4[Fe(CN)_6]$ ·$3H_2O$, 0.02 M X-Gluc) under 37°C

overnight. After staining, chlorophyll was washed by serial concentrations of ethanol.

For cleared tissue observation, the green siliques at and after flower position 6 were

collected and fixed in the fixation buffer (ethanol: acetic acid = 6: 1) for 4 h at room

temperature then post-fix samples in 100% ethanol and then 70% ethanol. At last,

samples were submerged in cleared buffer (chloral hydrate: glycerol: water = 8: 1: 2) for

overnight at room temperature and then observed and photographed with stereo

microscope (Zeiss).

Acquired Thermotolerance Assay

Chlorine gas sterilized seeds were grown on half-strength Murashige and Skoog (MS)

medium containing 0.8% Phytagel (Sigma-Aldrich) and 1% sucrose. The plates were

sealed with waterproof tapes and immersed in water bath at the indicated temperatures.

Samples were heated at 37°C for 1 h and then recovered at 22°C for 2 h before the

second 44°C lethal heat shock for 160 min. The survival rate of tested samples was

counted 10 d after heat treatment (Hsu and Jinn, 2010; Yeh et al., 2012).

31

Immunoprecipitation (IP) Assay and Western Blot Analysis

Nine-d-old seedlings were homogenized by a Dounce homogenizers (Sigma-Aldrich) with an immunoprecipitation (IP) lysis buffer (150 mM NaCl, 1 mM EDTA, 1% Triton X-100, 50 mM Tris-HCl, pH 7.4) with protease inhibitor cocktail (Roche). The protein-enriched extracts were collected after centrifugation at 12,000 rpm, 4°C for 20 min and quantified by the Bradford protein assay. For IP assay, 40 μL of ANTI-FLAG® M2 Affinity Gel (Sigma-Aldrich®) was used for each reaction with 1 mg protein extract. After incubated at 4°C on a rotary shaker overnight according to manufacturer's instruction, beads were washed 3 times, then boiled at 100°C for 10 min with 2.4x SDS sample buffer [125 mM Tris-HCl, pH 6.8; 4% SDS; 20% (v/v) glycerol, 0.004% bromophenol blue (BPB)] to elute IP samples.

Protein extracts were separated on 12.5% SDS-PAGE and transferred onto methanol washed 0.22 μm Immobilon® PVDF membrane (Millipore), then incubated with antibodies of α-FLAG (sc-807, SANTA CRUZ®; 1:3000), α-GFP (ab290, Abcam®; 1:5000) and α-actin (MAB1501, Millipore; 1:10000) in blocking solution. Horseradish peroxidase (HRP)-conjugated antibodies (1:10000) in TBST was utilized as secondary antibodies. Immobilon® Western Chemiluminescent HRP substrate (Millipore) was added for

32

chemiluminescent reaction and images were captured by KETA CL imaging system

(WEALTEC). Actin and Ponceau S stain were used as loading control for western blotting.

Liquid Chromatography Tandem-mass Spectrometry (LC-MS/MS) and Protein Identification Search

After IP, in-solution digesting, desalting followed by LC-MS/MS was performed at

the GLP Proteomics lab (Mass Solutions Technology). Samples were digested by trypsin

and underwent Orbitrap MS (Q Exactive, Thermo-Fisher Scientific) with a C18 column

(Thermo-Fisher Scientific). Tandem mass spectra were extracted by Proteome Discoverer

v1.4 (Thermo-Fisher Scientific) and searched through NCBInr_20150912,

TAIR10_20101214 and uniprot_2016.06 databases with Mascot v2.5 MS/MS Ion search

engine (Matrix Science). The following search parameters were specified: one missed

trypsin cleavage site was allowed, the parent ion tolerance and the fragment ion mass

tolerance were set at 10 ppm and 0.05Da, respectively. Carbamidomethyl (C) was chosen

as fixed modification while deamidated (NQ) and oxidation (N) were selected as variable

modifications. Exported Mascot DAT files were imported into Scaffold v.4.3 (Proteome

Software). Proteins were identified at both protein-identification probability > 95% and

at least 2 identified peptides with probability > 95% (Searle, 2010).

Coiled-coil Domain Prediction

Protein sequences were downloaded from the Universal Protein Resource (UniProt: http://www.uniprot.org) and coiled coils were predicted by use of the COILS program (http://www.ch.embnet.org/software/coils/COILS_doc.html) with non-weighted matrixes. A cutoff value of 21 amino acids minimum length was used for coiled-coil domain prediction and coiled-coil–forming probability was > 95%.

Scanning Electron Microscopy (SEM)

For silique observation, siliques at flower position 5 were collected and immediately observed on SEM (FEI, Inspect S) with low vacuum modes. Calculation of cell length was performed by the Image J software.

Chloroplast Photo-relocation Movement Assay

Induction and detection of chloroplast movement was analyzed by use of a 96-well microplate reader as described (Wada and Kong, 2011), with some modifications.

34

Chloroplast movement was induced in rosette leaves by applying different intensities of

blue light with an LED (wavelength peak 470 nm), then transmittance was measured at

660 nm. The light-induced transmittance changes were normalized to the transmission

level of the starting point.

Seed Protein Extraction

To examine protein profile of dry seeds, for each sample, 5 to 10 dry seeds were

used. First, seeds were grounded and mixed with 2x SDS sample buffer (2 mL 0.5 M Tris-

HCl, pH 6.8, 4 mL 10% SDS, 1.2 mL β-mercaptoethanol, 2 mL 100% glycerol, 0.8 mL ddH$_2$O

and 0.001% BPB) (Shimada et al., 2014). After centrifuged at 12,000 rpm for 15 min, 10

μL of protein-rich supernatant samples were separated on 13% SDS-PAGE gel, then the

gel was stained with Coomassie Brilliant Blue R-250 (Bio-Rad) for overnight and

destained with the mixture of ddH$_2$O, methanol, and acetic acid in a ratio of 50: 40: 10

(v: v: v). The image was captured by FluorChem M system (Proteinsimple®).

Mutagenesis Construct with Megapriming Method

The HSBP heptad repeat region point mutations lines were performed by

Megapriming method (Barik, 2002). The designed primer sets sequences are listed in

Table 1.

Transient Expression Assay in Arabidopsis Mesophyll Protoplasts

Three to four weeks-old Arabidopsis leaves were cut to thin strips then transferred

into freshly prepared enzyme solution (1.5% cellulase R10, 0.4% macerozyme R10, 0.4

M mannitol, 20 mM KCl, 10 mM $CaCl_2$, 20 mM MES, pH 5.7) and kept in dark for 4 to 5 h

after vacuumed. Protoplasts were harvested and washed by W5 solution (154 mM NaCl,

125 mM $CaCl_2$, 5 mM KCl, 5 mM glucose, 2 mM MES, pH 5.7) then briefly centrifuged.

200 μL of the MMG solution (0.4 M mannitol, 15 mM $MgCl_2$, 4 mM MES, pH 5.7) was

used to resuspend the collected protoplasts from each reaction (at least 2 x 10^4

protoplasts) and mixed gently with 10 to 40 μg of plasmid DNA and 220 μL PEG solution

(40 % PEG4000, 0.2 M mannitol, 0.1 M $CaCl_2$) at room temperature for 10 min followed

by 800 μL of W5 solution added into mixture to cease the reaction. Finally, protoplasts

were collected and resuspended in 1 mL of W5 solution in a 6-well tissue culture plate,

then incubated at 22°C for 14 to 16 h (Yoo et al., 2007).

For the GFP or YFP signal observation, 9 μL of protoplast solution mixed with 1 μL

of DAPI (2 μg/μL) and examined by confocal microscope (Zeiss LSM 780 Confocal). The GFP, YFP, DAPI and chlorophyll auto-fluorescence signals were detected with 488 nm, 495-510 nm, 359 nm and 630 nm excitation and 505-530 nm, 520-550 nm, 461 nm and 680 nm emission, respectively.

For cycloheximide (CHX) treatment, transformed protoplasts were incubated overnight for 14 to 16 h at 22°C then subsequently treated with CHX at a concentration of 100 μg/mL and further incubated for 1.5 to 2 h under room temperature. After the CHX treatment, protoplasts were treated with mild 37°C heat treatment for 30 min followed by 1 h and 3 h recovery (Weber et al., 2008; Machettira et al., 2012).

For native-PAGE analysis, at least 4 x 10^5 protoplasts were used for each sample. Collected transfected protoplasts were added with adequate GM buffer (150 mM Tris-HCl, pH 7.2) or IP lysis buffer (150 mM NaCl, 1 mM EDTA, 1% Triton X-100, 50 mM Tris-HCl, pH 7.4) to break the cell membrane. After centrifugation, clear supernatant was mixed with the 10 x native dye (50% glycerol, 0.01% BPB) and separated on 15% native-PAGE gel then transferred onto methanol washed 0.22 μm Immobilon® PVDF membrane (Millipore), then incubated with antibodies of α-FLAG (sc-807, SANTA CRUZ®; 1: 3000). HRP-conjugated antibodies (1: 10000) in TBST was utilized as secondary antibodies.

37

Immobilon® Western Chemiluminescent HRP substrate (Millipore) was added for

chemiluminescent reaction (WEALTEC).

Statistical Analysis

Data are presented as one of at least three independent experiments. Statistical

analysis involved Student's *t* test (Two-tailed, paired). *P* value < 0.05 was considered as

statistically significant.

Primers and Accession Numbers

Sequence data in this article can be found in The Arabidopsis Information Resource

(TAIR) database under the following accession numbers: HSFA1a (At4g17750), HSFA2

(At2g26150), HSP101 (At1g74310). CIP1 (At5g41790), CIP1L (At1g64330), HSBP

(At4g15802), KAC1 (At5g10470), KAC2 (At5g65460), MAG2 (At3g47700), MIP1

(At2g32900), MIP2 (At5g24350), MIP3 (At2g42700).

RESULTS

Histochemical Analysis of the Arabidopsis *HSBP* Expression

The expression of Arabidopsis *HSBP* in response to HS has been shown preferentially in different tissues by qRT-PCR analysis (Hsu and Jinn, 2010; Hsu et al., 2010).

To elucidate the expression profile of *HSBP* at the developmental stages, transgenic plants harboring a 1.5 kb potential *HSBP* promoter fused with a reporter *ß-glucuronidase* (*GUS*) gene was analyzed. The results of histochemical analysis showed that GUS activity was weak in the 12-d-old seedlings and mainly observed in the leaf vein, the petals, the filament of anthers, the apex and basal of nascent siliques and the valves and septum of the mature siliques **(Figure 1A, C to E)** The GUS activity was undetectable in the roots of 7-day-old seedlings **(Figure 1B)**.

GUS activity in 12-day-old seedlings when treated with 37°C for 1 h was higher **(Figure 2A)**, indicating that the expression of HSBP promoter was induced by heat. However, the GUS activities in the flowering clusters, root and silique tissue were not affected by the heat treatment **(Figure 2B to D)**.

The Characterization of *HSBP* Complementation Transgenic Plants

The 1.5 kb *HSBP* potential promoter region along with the *HSBP* gene fused with

3xFLAG at C-terminal was transformed into *hsbp* mutant plants, and four independent

complementation lines were characterized **(Figure 3A)**. The transgene expression was

verified by RT-PCR and western blotting analyzed with α-FLAG antibodies. Then, shorten

silique length and seed abortion phenotypes of *hsbp* were rescued **(Figure 3B)**, similar

to the *35S::HSBP-3xFLAG* transgene as our previous results (Liu and Jinn, 2014).

The Identification and Verification of Potential HSBP-interacting Proteins

To discover the potential function of HSBP in Arabidopsis development stages. The

35S::HSBP-3xFLAG/hsbp and *proHSBP::HSBP-3xFLAG/hsbp* transgenic plants were

subjected to the immunoprecipitation (IP) assay followed by LC-MS/MS assay to identify

the potential HSBP-interacting proteins.

The MS data showed that both normal condition and after the heat treatment,

proHSBP::HSBP-3xFLAG detected TGG2 (glucoside glucohydrolase, At5g25980) with 14%

coverage as one of the possible candidates but with only 4 exclusive unique peptides

and spectra were counted. However, the results from the *35S::HSBP-3xFLAG* plants after

heat treatment illustrated that multiple possible candidates were identified with at least

10 exclusive unique peptides and spectra counts for each hits. Combined the two sets of

MS results, we then concluded that HSBP was most likely to have physical interactions

with CIP1 (COP1-interactive protein 1), CIP1-like (CIP1L), KAC1/2 (Kinesin like protein for

action based chloroplast movement 1/2), MAG2 (Maigo2, seed storage protein), ZW10

(Putative centromere/kinetochore protein), Sec39 (Secretory pathway 39), and putative

Sec-1 like domain-containing protein **(Table 2)** since that each of them has high exclusive

unique peptides and spectra counts (Liu and Jinn, 2014). The low expression level of

HSBP in the native promoter complementation transgenic plants was expected and was

consistent with the GUS activity results **(Figure 1)**.

According to our previous BiFC results, the reconstituted YFP signal was observed

evenly distributed in the cytoplasm when HSBP co-expressed with KAC1, MAG2, CIP1L,

HSP70-3, and HSBP itself. CIP1L protein was considered as a representative of CIP1 since

it exhibited high sequence similarity (71%) compared to the CIP1 (Liu and Jinn, 2014). To

verify the interactions between HSBP and the IP-identified candidates, the Co-IP assay

were both performed to further assess the interactions **(Figure 4)**.

Apart from the BiFC confirmations (Liu and Jinn, 2014); when *HSBP-3xFLAG*

transgene co-expressed with the *GFP-KAC1*, *-MAG2*, or *-CIP1* plasmids, the Co-IP result showed that all three candidates were HSBP interacting proteins **(Figure 4)**.

HSBP is a small 10-kDa protein comprising a sole coiled-coil motif, thus the interacting ability of HSBP was due to the coiled-coil domain; therefore, all HSBP-interacting protein sequences were analyzed with COILS prediction program. The prediction results showed that all candidates harbored at least one sequence area with > 95% possibility to be a coiled-coil domain **(Appendix 1)**.

The *mag2* and *cip1* Mutant Identification and Characterization

To evaluate the relationship between HSBP and HSBP-interacting proteins in the heat response. The *mag2* (SALK_037370) and *cip1* (SAIL_841_A08) mutant were identified and verified by genotyping PCR **(Figure 5A)** and the RT-PCR **(Figure 5B and C)**. The *kac1, kac2,* and the *kac1kac2* double mutants were provided by Dr. Masamitsu Wada of Kyushu university (Suetsugu et al., 2012; Shen et al., 2015).

The acquired thermotolerance assay was performed on *mag2*, *cip1*, *kac1, kac2,* and *kac1kac2* mutant plants **(Figure 6)**. The *hsbp* and *cip1* mutants showed significantly 40% better survival rate than the WT (Col) but had no effects on *mag2*, *kac1, kac2,* and

kac1kac2 mutants. The heat-sensitive *hsp101* mutant was considered as a reference. The results implied that the CIP1 was also a possible negative regulator during the HSR.

To furthermore examine the relationships between HSBP and HSBP-interacting proteins, the gene expression profile of HSBP-interacting-proteins in response to heat stress were examined **(Figure 7)**.

We thus analyzed the HSBP-interacting gene expression level in response to HS by q-PCR in WT and *hsbp* mutant **(Figure 7A)**. In WT plants, the *MAG2* expression was distinctly upregulated at the 22°C recovery stage after a mild 37°C HS for 1 h, and at the 44°C lethal HS, as well as the final recovery stage. The results were consistent with the previous reports stated that the *MAG2* was essential in the thermotolerance response (Zhao and Lu, 2014). While in *hsbp* mutant, the *MAG2* and *KAC1* showed higher expression levels than the WT under normal growth condition, while all three tested genes were significantly downregulated at the lethal heat stress and the final recovery stage.

The *cip1* showed a higher thermotolerant phenotype **(Figure 6)**. We furthermore found that the expression level of HSBP was significantly downregulated in the *cip1* mutant at the lethal HS **(Figure 7B)**. Then, the HSR-positive marker genes *HSFA1a, HSFA2,*

and *HSP101* were all significantly upregulated **(Figure 7C)**. The result was consistent with the higher survival rate of the *cip1* mutant compared to the WT.

Subcellular Localization of HSBP-interacting Proteins

In order to uncover the potential functions of HSBP in associated with the identified interacting proteins, we examined the subcellular localizations of HSBP-interacting proteins **(Figure 8)**.

In WT protoplast **(Figure 8A)**, the MAG2-GFP was observed majorly localized at the endoplasmic reticulum (ER), which was consistent with the previous findings showed that the MAG2 is involved in the seed storage protein transportation on the ER (Li et al., 2006; Zhao et al., 2013). CIP1-GFP was reported to associate with the cytoskeleton in hypocotyl and cotyledon cells by immunofluorescent labelling analysis (Matsui et al., 1995; Ren et al., 2016). Our results showed that CIP1-GFP scattered in the cytoplasm and a small part of CIP1 located to the nucleus **(Figure 8A)**. Previous studies revealed that the distribution patterns of KAC1 and KAC2 were very similar to the pattern of cytosolic cytoskeleton (Suetsugu et al., 2012; Shen et al., 2015); however, based on our observation, KAC1 protein dispersed in the cytoplasm and presented as dots pattern in

44

WT. Also, a large proportion of KAC proteins were observed to localize in the nucleus in

WT protoplasts.

In *hsbp* protoplasts **(Figure 8B)**, the subcellular localization of tester-GFP signals

showed that there were no major differences compared to WT; excepted for the

nucleocytoplasmic distribution pattern of CIP1 and KAC1 were altered. This suggested

that HSBP may participates in the protein distribution mechanism through coiled-coil

domain interactions.

The localization of HSBP in the HSBP-interacting proteins mutant lines were also

examined **(Figure 9)**. The HSBP-YFP mainly localized in the cytoplasm and translocated

into the nucleus in response to the HS (Hsu and Jinn, 2010; Hsu et al., 2010). The HSBP-

YFP in the *mag2* and *cip1* mutants was observed in the nucleus; suggested that the

distribution pattern of the HSBP was affected in the absence of *MAG2* and *CIP1* genes.

Versatile Effects of HSBP on Arabidopsis Development Stages

It has been well characterized that the light controlled CONSTITUTIVE

PHOTOMORPHOGENETIC1 (COP1) nuclear-cytoplasmic partitioning is tightly regulated

by the CIP1 (Matsui et al., 1995). COP1 is a ubiquitin E3 ligase that integrates signals from

various photoreceptors and also controls many downstream light-regulated genes

expressions (Osterlund et al., 1999; Jang et al., 2015). In Arabidopsis, CONSTANS (CO) is

a pivotal positive regulator of flowering. Under the long-day conditions (LDs), highest *CO*

mRNA accumulation occurs in the afternoon and activates transcription of *FLOWERING*

LOCUS T (*FT*) gene in leaves. FT then functions as a florigen and migrates from leaves to

the shoot apex to induce the downstream flowering genes expression (Baurle and Dean,

2006; Fornara et al., 2010; Wellmer and Riechmann, 2010; Golembeski and Imaizumi,

2015). In addition, COP1 functions as a repressor to promote the ubiquitin-mediated

proteolysis of CO in darkness, and blue-light photoreceptor cryptochrome 1 (CRY1)

negatively regulates COP1 thereby stabilizing the CO activity (Osterlund et al., 1999; Liu

et al., 2008; Lau and Deng, 2012; Jang et al., 2015; Park et al., 2017).

Here, to understand the molecular mechanisms of early flowering phenotype in

hsbp mutant **(Figure 10A)**, as pervious reported by Hsu et al. (2010). We analyzed the

flowering pathway marker genes expression by qRT-PCR in the *hsbp* and WT plants

(Figure 10B).

The *CIP1* and *COP1* expression levels were significantly reduced whereas *CO* and

CRY showed higher expression levels; therefore, subsequently the downstream *FT*

expression level was upregulated in the *hsbp*, as compared to the WT. Since CIP1

mediates COP1 nucleocytoplasmic distribution and has physical interaction with HSBP.
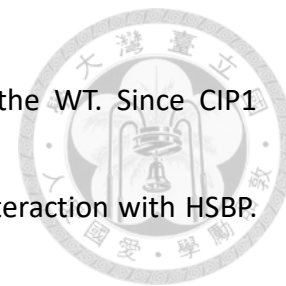
We thus subjected the WT and *hsbp* to different light sources, followed by conducting

the photomorphogenesis assay to evaluate the possible physiological effects of HSBP on

photoresponses **(Figure 10C)**.

The 3-d-old *hsbp* mutant showed the significantly arrested hypocotyl elongation

length under red (6.34 µmol m^{-1} s^{-1}) and blue (5.08 µmol m^{-1} s^{-1}) light by 30% and 26%

shorter, respectively, compared to the WT; but was unaffected under the dark condition

(Figure 10C). The *35S::HSBP-3xFLAG* transformed lines complemented the *hsbp* mutant

phenotype showed similar phenotype as the WT. From the qPCR data obtained, here I

proposed the flowering signal pathway regarding to HSBP. HBSP cooperated with CIP1 to

regulate the activity of downstream gene *COP1*. In the absence of HSBP, the expression

level of both *CIP1* and *COP1* were weaker than usual, which causing higher expression

level of *CO* and furthermore stimulating the flower integrator gene FT then ultimately

promoted the flowering **(Figure 11)**.

The short-silique phenotype has been characterized in the *hsbp* mutant (Hsu et al.,

2010); here, the cell length of silique was significantly affected in the *hsbp* **(Figure 12A**

47

to C). Interestingly, the cells of root, hypocotyl, leaf epidermal, stem, septal and petal were not affected **(Appendix 2)**.

It has been reported that MAG2, MIP1, and MIP2 formed a tethering complex localized on the ER membrane and was responsible for efficient transport of seed storage proteins, which was similar to the yeast Dsl1p-Sec39p-Tip20p complex and the mammalian RINT1-ZW10-NAG complex (Li et al., 2013; Zhao et al., 2013; Tagaya et al., 2014). Studies also shown that in Arabidopsis *mag2* mutant accumulated abnormal precursors of two major seed storage proteins, 2S albumin and 12S globulin, in dry seeds. *mip* mutants also exhibited the similar aberrant accumulation (Shimada et al., 2003; Li et al., 2006; Li et al., 2013; Zhao et al., 2013).

Previous LC-MS/MS results contributed by Liu and the Co-IP validation confirmed that HSBP interacted with MAG2 (At3g47700), AW10 putative centromere/kinetochore protein (At2g32900), Sec39 (At5g24350), and putative Sec-1 domain-containing protein (At2g42700), as well as the MIP1 (MAG2-interactive protein 1), MIP2 and, MIP3, respectively **(Table 2)**.

The one-third ratio of seed abortion phenotype was also observed in the *hsbp* mutant (Hsu et al., 2010). Here, we analyzed the seed protein profiles of *hsbp* in

comparison with the WT, *mag2*, HSBP-complementation, and HSBP-overexpression line **(Figure 13)**. The immunoblotting result collaborated with Drs. Hara-Nishimura and Shimada showed that the abnormal seed precursor proteins 2S albumin (p2S) and 12S globulin (p12S) were detected in the *mag2* and the mis-shaped *hsbp* (*hsbp-b*) seeds **(Figure 13)**. The seed length of *hsbp-b* was also significantly shorter than the WT **(Figure 14)**.

The chloroplast movement assay showed that the protoplasts in *hsbp* mutant had slower velocity of both accumulation and avoidance movements **(Appendix 3)**, indicating the possibility that the HSBP also interacted with other components of the chloroplast movement complex, e.g., KAC1 and 2.

The Effects of HSBP Heptad Region Point Mutations on HSBP Oligomerization Status

The heptad repeat is a structural motif that consists of a repeating pattern of seven amino acids and result in a coiled-coil domain. In HSBP, the heptad repeat coiled-coil is crucial for the structure and the function because it is the only functional domain of HSBP. The first and fourth residue of the se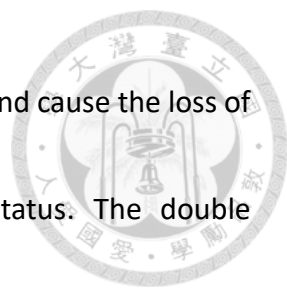ven repeating amino sequence (i.e. "***a***" and "***d***" in the sequence of ***abcdefg***) are typically nonpolar core residues to maintain the

49

interhelical interface and to shape the overall oligomerization state of the coiled-coil

domain, whereas "*e*" and "*g*" are solvent-exposed, polar residues that give specificity

between the two helices through electrostatic interactions **(Appendix 4)** (Mason and

Arndt, 2004; Truebestein and Leonard, 2016).

The previous study on the human HSBP1 (hHSBP1) revealed that each single-helix

of hHSBP1 formed coiled-coil homo-trimers with other parallel helices; furthermore, the

two hHSBP trimers assembles in a head-to-head fashion into hexamer form **(Appendix

5)** (Liu et al., 2009). In the three-helix bundle region of HSBP1, an anomaly occurs at the

conserved serine 31 (Ser31), which occupies the position where methionine 30 should

be according to the heptad repeat pattern prediction. This side chain of Ser31 shares the

hydrogen bond with the phenylalanine 27 (Phe27) from the previous helical turn

indicating that this conservation of Ser31 is likely to bear some biological functions.

The preceding studies reported that the substitution of Ser31 to alanine would

compromise the ability of cytoplasmic-nucleus translocation in Arabidopsis (Hsu and

Jinn, 2010), but not the ability to bind with HSFs in maize (Fu et al., 2006; Liu et al., 2009).

The observed hexameric helix bundles were validated by the disruption of hexamer

structure in hHSBP1. A double mutation I34R/I38R was created in the center area of the

coiled-coil region. These Arg residues would repel from each other and cause the loss of

ability to oligomerization, thus the tendency for monomeric status. The double

mutations L12D/V15D introduced in the trimer-trimer interface also prevent the

formation of hexamers; whereas the T13C variant is a type of conservative mutation,

which ultimately causing the stronger connection between two homotrimers (Fu et al.,

2006; Liu et al., 2009).

To understand if the corresponding mutations in Arabidopsis have the similar

structural effects. The transgene of these *HSBP* (mutant formats)-*3xFLAG* were

transformed into WT protoplasts, then the partition changes of HSBP oligomerization

status (i.e., monomer, trimer, and hexamer status) were observed by native-PAGE
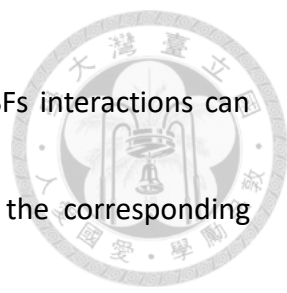
analyses **(Figure 15 and 16)**.

The results showed that the M16D/V20D and I38R/I42R mutations completed loss

of the hexamer status **(Figure 16A, Lanes 5 and 7)**, which were consistent with the effect

on hHSBP1; however, the I38R/I42R still remained the ability for oligomerization **(Figure

16A, Lane 7)**. Meanwhile, it has not yet been reported M16D/F19D variation showed the

same effect as the M16D/V20 conserved mutant **(Figure 16A, Lane 5 and 6)**. Interestingly,

the population of oligomerization of the HSBP showed a relatively low status of trimer

51

(Figure 16A, Lane 2), as compared to the previous studies on hHSBP1 (Liu et al., 2009).

It has been reported that hHSBP-T13C mutation results in a significantly increase of the

hexamer status (Liu et al., 2009). We thus generated HSBP-T17C mutation and the results

agreed with the finding of hHSBP-T13C, compared to the HSBP **(Figure 16A, Lanes 2 and**

4).

Previous studies on the maize HSBP homologs EMP2 (HSBP1) and HSBP2 indicating

that multiple mutations HSBP2-I52K/M55K and -I59K/L62K in the coiled-coil region

disrupts the ability of HSBP2 to interact with HSFA4a and the HSFA4a mutants harboring

the similar amino acid mutation in the HR regions also lost the ability to interact with

HSBP2, based on the results of yeast-two hybrid (Fu et al., 2006).

In summary, the hetero-oligomerization of HSBP2 and HSFA4a was determined by

the hydrophobic interactions between their coiled-coil domains has been reported (Fu

et al., 2006). Furthermore, the replacement of the "*g*" position arginine 58 with lysine

(R58K) also interrupted the interaction between HSBP2 and HSFA4a. This suggested that

the attractive electrostatic interaction between "*e*" and "*g*" residues were also

important for the stability and the function of the coiled-coil domains (Satyal et al., 1998;

Fu et al., 2002; Tai et al., 2002; Liu et al., 2009).

To understand if the HSBP mutations that the interrupted HSFs interactions can cause structural and physiological effect changes in Arabidopsis, the corresponding Arabidopsis mutations HSBP-R48K, -I42K/M45K, and -I38R/I42R/I49K/L55K were generated **(Figure 16A, Lanes 3, 9, and 11)**. The results showed that the HSBP-R48K mutation caused an increase of the trimer proportion of the HSBP **(Figure 16A, Lane 3; Figure 14B, Lane 2)**.

The HSBP-I42K/M45K mutation **(Figure 16A, Lane 9)**, the migration of HSBP was detected at the position between the status of trimer and hexamer. The quadruple HSBP-I38R/I42R/I49K/L55K mutation **(Figure 16A, Lane 11)** was generated to attempt to completely break down the capability to form oligomer, and the result showed a similar effect as the I45K/M45K mutation on the HSBP structure change.

Previous study conducted on human parasite *Plasmodium falciparum* HSBP (PfHSBP) oligomerization has been pointed out that the PfHSBP was highly likely to be sodium dodecyl sulfate (SDS) resistant (Sayeed et al., 2014). Thus, we assessed the mutant of HSBP-R48K (trimer-status) and -T17C (hexamer status) in SDS-PAGE to determine whether Arabidopsis HSBP was also SDS-resistant **(Figure 16B)**.

Notably, the samples did not subject to SDS and heat pretreatments before spread

in an SDS-PAGE. The MW of the HSBP-R48K and -T17C was detected approximately 30

kDa and 70 kDa, respectively **(Figure 16B, Lanes 2 and 3).** The result was consistent with

the previous studies of SDS-PAGE analysis performed on PfHSBP indicating trimeric and

hexametric forms ran about at sites of 30 kDa and 70 kDa, respectively (Sayeed et al.,

2014).

To examine the possible physiological effects of the HSBP mutations, the transgenic

lines of the GFP-fused HSBP-I42K/M45K and -I49K/L52K mutant generated in *hsbp*

background by (Hsu et al., 2010) were tested with acquired thermotolerance assay

(Figure 17). The results revealed that the HSBP-I42K/M45K and -I49K/L52K mutants

exhibited a higher thermotolerance compared to the WT, similar to the heat resistant

phenotype of the *hsbp.*

To examine the partition of the HSBP monomer, trimer and hexamer forms in

Arabidopsis in response to HS, the *35S::HSBP-3xFLAG* transformed protoplasts were

subjected to cycloheximide (CHX) treatment before treated with mild 37°C 30 min HS

following the 22°C 3 h recovery **(Figure 18)**.

The western blotting result of native-PAGE showed that under the HS and during

the recovery from HS (attenuation of the HS response), the intensity of HSBP hexamer

signal was significantly reduced; the HSBP-hexamer signal was undetectable after 3 h

recovery for the HS **(Figure 18A)**. Meanwhile, the SDS-PAGE results revealed that the

total amount of HSBP remained the same before and after the HS treatment (**Figure 18B**).

Conclusions

Being a small protein, HSBP had proven to have versatile function regarding to the

heat shock response and development stages of Arabidopsis. By cooperating with the

MAG2 complex, HSBP can affect the process of intramembrane protein trafficking and

influent the seed protein accumulation. However, the abnormal seed protein

accumulation observed in the *hsbp* mutant dry seeds was not the primary reason behind

the seed abortion phenotype in *hsbp*. HSBP can also play roles in both flowering time

control and photomorphogenesis by regulating the function of COP1 through binding

with the interactive protein of COP1, CIP1. HSBP might also participate in the regulation

of chloroplast movement by affecting the KAC1/2 proteins **(Figure 19)**.

DISCUSSION

**Heat Shock Factor Binding Protein and the Coiled-coil Domain**

Heat shock factor binding protein (HSBP) was first identified in human as HSBP1 and functioned as a repressor during the heat shock response (HSR). HSBP1 homolog of EMP2 (i.e. HSBP1), HSBP2, as well as of *Os*HSBP1 and *Os*HSBP2 are found in the maize and rice, respectively; notably, the HSBP1 homolog was not found in yeast. Our previous study identified that the only one HSBP1 homolog was found in Arabidopsis, AtHSBP, and characterized it as a repressor in HSR (Hsu et al., 2010).

The coiled-coil domain of HSBP1 has been proven to interact with the heptad repeat regions (HR-A/HR-B) of HSF and to detach the HSF from HSE of HSP to attenuate the HSR. This phenomenon is also observed and verified in the maize, rice, and Arabidopsis (Satyal et al., 1998; Fu et al., 2006; Hsu and Jinn, 2010; Hsu et al., 2010; Rana et al., 2012; Sayeed et al., 2014). Since coiled-coil domain is the only functional domain in HSBP, thus its ability to attenuate HSR could also be contributed to the coiled-coil domain interaction.

In Arabidopsis *hsbp* mutant, other than the expected enhanced HSR phenotype, three distinct phenotypes were also observed, including the early flowering, shorten silique length, and the one-third ratio of seed abortion. These phenotypes suggested

56

that HSBP was much more functional versatile than we previously understood.
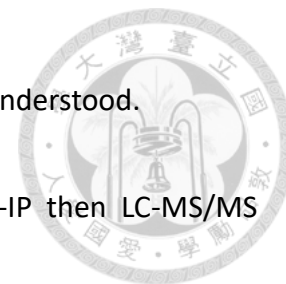
We have identified the interacting proteins of HSBP by Co-IP then LC-MS/MS analysis. The interacting proteins including cytoskeleton-associated proteins CIP1, CIP1L, KAC1/2, and the ER-localized proteins MAG2, MIP1, 2, and 3 **(Table 2)**. These interacting proteins all exhibited at least one coiled-coil domain and we have observed that the coiled-coil domain deleted MAG2 loss the ability for HSBP interaction, indicating that the interactions between HSBP and its interacting proteins relied on the coiled-coil domain interactions (Hsu and Jinn, 2010; Hsu et al., 2010).

The repeating seven amino acids ("*abcdefg*") determine the nature of coiled-coil domain oligomerization status, the "*a*" and "*d*" residues must be hydrophobic to stabilize the helix structure through Van der Waals interactions, and the charged residues "*e*", "*g*" form interhelical electrostatic interactions (Mason and Arndt, 2004; Truebestein and Leonard, 2016). Previous studies on human revealed the hexamer structure of HSBP1 in a "head-to-head" trimer fashion and indicated that mutated amino acids in the heptad repeats could result in the alterations of oligomerization status (Liu et al., 2009).

For instance, the substitution of this Ser31 with isoleucine residue (S35A) would enhance the stability of the HSBP1 trimer but sacrifice some of its functions and

I34R/I38R would loss the ability to oligomerize. The study of *Plasmodium falciparum* stated that PfHSBP exhibited certain level of SDS-resistance and both trimer form and hexamer form HSBP existed under normal condition (Sayeed et al., 2014).

Our research on Arabidopsis also revealed the importance of the coiled-coil domain. The HSBP-S35A variant could not translocate into the nucleus when heat stress occurred (Hsu et al., 2010). The HSBP-T17C and -R48K mutations have been shown to affect the oligomerization status but whether it has effects on physiological phenotype changes were not observed yet. The transgene constructs HSBP-I42K/M45K and -I49K/L52K expressed in *hsbp* background could not complement the *hsbp* mutant phenotype but showed higher survival ratio after subjected to the acquired thermotolerance assay, similar to the *hsbp* mutant **(Figure 17)**. In conclusion, structural alterations of HSBP conserved heptad repeat region can indeed have influences on physiological functions.

Cycloheximide (CHX) is a eukaryote protein synthesis inhibitor that can interfere the translocation step of protein synthesis, thus block the translation process (Machettira et al., 2012). In this study, for the purpose of evaluating the oligomeric-status changes of HSBP in response to HS to preliminarily determine the function of each structural form of HSBP, the native-PAGE analyses were conducted. According to the native-PAGE

analyses results, all three forms of HSBP existed at the same time while the trimer form

HSBP having the largest proportion at the initial equilibrium state **(Figure 18A)**. Judging

from the SDS-PAGE results, I assumed that the total amount of HSBP did not significantly

change. Therefore, with the progression of HS and the following recovery, we deduced

that the hexamer form HSBPs served as the inactive form in cytoplasm and gradually

disassembled into active trimer form when HS occurred.

The HSBP and the Chloroplast Photo-relocation

Chloroplast photo-relocation movement is the process which the chloroplasts

migrate within cells to avoid photo-damaged or to perceive light more efficiently by

attaching to actin filaments. Recent studies on Arabidopsis reported that it is the short

actin filaments surrounding the chloroplasts (cp-actin) that were involved in the

chloroplast movement and attached with the plasma membrane rather than the

cytoplasmic actin cables (Suetsugu and Wada, 2007; Wada, 2016).

The molecular components regulating this cp-actin movement are well

characterized. Two types of proteins, KAC (KAC1 and KAC2) and CHUP1 proteins were

identified as the necessary components for the existence of cp-actin filaments and both

of them were coiled-coil domain harboring proteins. Both *kac1 kac2* and *chup1* mutants

completely lacked the presence of cp-actin filaments but retained the normal

cytoplasmic actin filaments, indicating that KAC and CHUP1 proteins are vital for the

formation and maintenance of cp-actin filaments (Woehlke and Schliwa, 2000; Suetsugu

et al., 2012; Shen et al., 2015).

Two other coiled-coil proteins, WEB1 and PMI2 were also discovered as the factors

that mediated light-induced cp-actin filaments reorganization. WEB1 and PMI2 had been

reported to interact with each other in yeast and plant cells to form large complexes.

Studies revealed that WEB1 and PMI2 controlled the chloroplast movement velocity

(Kodama et al., 2010). In *hsbp* mutant, the velocity of chloroplasts movement was slower

than in WT under both accumulation and avoidance conditions **(Appendix 3)**. Since we

already knew that HSBP is also the coiled-coil domain harboring protein and has

interactions with the KAC proteins, HSBP is most likely to participate in the chloroplast

movement mechanism.

CIP1 and HSBP, the Possible Crosstalk Between Photomorphogenesis and Heat Stress

Signal Transduction

Light and temperature are arguably two of the most important environmental signals regulating the growth and development of plants (Bhattacharya et al., 2017). In addition to their fundamental effects on regular plant growth, perceptions of light and temperature changes also provide vital instantaneous responses to ensure the optimal development. There is increasing evidence for considerable crosstalk between the heat stress response and light signal transduction. In Arabidopsis, B-box zinc finger protein BBX18, a negative regulator in photomorphogenesis is also a negative in thermotolerance and weaken the HSR (Wang et al., 2013; Franklin et al., 2014).

COP1 is a RING E3 ubiquitin ligase that acts as the central integrator in the light signal pathway, where itself mediated by the photoreceptors and promotes the ubiquitination and degradation processes. Integrating signals from various photoreceptors, COP1 manipulates photomorphogenesis through targeting several transcription factors by a Ub-proteasome system (Osterlund et al., 1999; Jang et al., 2015; Park et al., 2017). In the darkness, COP1 aims effectors ELONGATED HYPOCOTYL 5 (HY5), LONG AFTER FAR-RED LIGHT 1 (LAF1) and LONG HYPOCOTYL IN FAR RED 1 (HFR1) for ubiquitination and degradation, then suppresses of the photomorphogenesis, while in the presence of light, activated photoreceptors repress COP1 function and promote

61

photomorphogenesis-enhancing transcription factors, then leading to the proper

photomorphogenesis development. CIP1 has been reported to control the

nucleocytoplasmic distribution of COP1 and sequestrated COP1 in the cytoplasm under

light condition to facilitate photomorphogenesis (Osterlund et al., 1999; Jang et al., 2015;

Park et al., 2017). We have identified CIP1 as the interacting protein of HSBP and strongly

strengthen HSR is observed in the *cip1* mutant **(Figure 7B and C)**, while *hsbp* exhibits

shorter hypocotyl length under red light and blue light conditions **(Figure 10C)**,

suggesting that CIP1 and HSBP are both involved in the light signal transduction and the

HSR. In conclusion, the interaction between HSBP and CIP1 may be the newly discovered

crosstalk between photomorphogenesis and the HSR.

The Seed Abortion of *hsbp* Mutant

One-third ratio of seed abortion phenotype was observed and characterized (Liu

and Jinn, 2014). The MAG2 complex, which comprised of MAG2, MIP1, MIP2, and MIP3,

has been proved to be essential for the seed proteins intracellular trafficking (Li et al.,

2006; Li et al., 2013). Our Co-IP and LC-MS/MS results showed that HSBP interacted with

all four members of the MAG2 complex. The abnormal precursor proteins of 12S

62

globulins and 2S albumins were discovered in the *mag2* mutant as well as in the *mip1*, *mip2,* and *mip3* mutants (Li et al., 2013). From the immunoblotting results provided by Drs. Hara-Nishimura and Shimada, the misshapen *hsbp* seeds (*hsbp-b*) also detected with traces of p12S and p2S **(Figure 13 and 14)**. However, the *mag2* mutant did not exhibit the similar seed abortion phenotype suggesting that in spite of the interaction between HSBP and MAG2 complex, it might not be the fundamental reason of the seed abortion in *hsbp*.

The embryo-defect or embryo-lethal mutants of Arabidopsis had been well studied. These defective mutants were often accompanied with various phenotypes, such as arrested development, color changes of embryo or aborted seeds (Heath et al., 1986). Since the storage proteins only started to accumulate at the late stages of embryo maturation process and the accumulation of seed storage proteins was already tied to the morphogenetic changes occurred during the embryo development, the seed abortion phenotype of *hsbp* might be the result of the arrested embryo development of *hsbp* plants.

Perspective and Future Work

From the current studies, we can conclude that Arabidopsis HSBP interacts with proteins to mediate the downstream growth and development processes, whereas the mutant lines of HSBP-interacting proteins exhibit gene expression level alterations and phenotype changes in response to the heat stress, indicating the coordinating relationship between HSBP and its interacting proteins. However, whether they function dependently or being redundant with each other remain unknown. Therefore, the double mutants line *hsbp mag2* and *hsbp cip1* should be created to answer the question.

We now decipher the preliminary roles of HSBP in various development stages. First, HSBP involves in the photomorphogenesis and flowering signal pathway by interacting with CIP1 then affects the expression and sensibility of COP1. Second, HSBP involves in the chlorophyll photo-relocation movement by interacting with KAC1 and KAC2. However, despite that the interaction of HSBP and the MAG2 complex is confirmed, the role of HSBP in the process of proper seed development remain unclear. Therefore, factors other than seed protein should also be considered.

The coiled-coil domain is the only functional domain of HSBP suggesting its importance for both the physiological function and the oligomerization status. Under
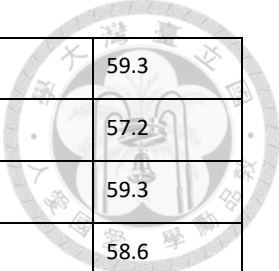
the normal condition, hHSBP1 exhibits both the trimer and hexamer forms according

previous studies (Liu et al., 2009). Although we have observed the changes

corresponding to the point mutations in the heptad repeat region of hHSBP1 and maize

HSBP2, the exact oligomerization status of each mutation form still largely unrecovered.

Despite that we observed the partition changes of HSBP in response, the size exclusion

chromatography should be conducted to determine the exact structure in each stage

and also the mutated HSBPs.

TABLES
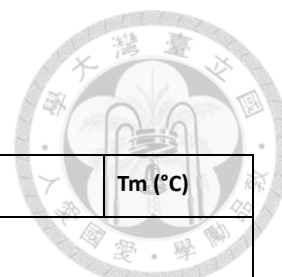
Primer	Sequence (5' – 3')	Tm (°C)
Genotyping		
MAG2-Genotyping-Fw	AGCACCACCAGATTTCATCAG	52.4
MAG2-Genotyping-Rv	GCAGACTTTACCGCTATGTGG	54.4
CIP1-Genotyping-Fw	TCTCAGCTCCTCATCAAGCTC	54.4
CIP1-Genotyping-Rv	GTGGAATCAGCAGAGGAACAG	54.4
pROK2 LB 1.3	ATTTTGCCGATTTCGGAAC	52.8
pDAP101	GCCTTTTCAGAAATGGATAAATAGCCTT	55.4
Cloning		
proHSBP-BamHI-Fw	<u>GGATCC</u>AATTGGAATTTGCTCTTG	54
proHSBP-EcoRI-Rv	<u>GAATCC</u>TTTTAGGGTTTTCTTGCGA	54.4
HSBP-CDS-Fw	ATGGATGGTCATGATTCTGAG	50.5
HSBP-CDS-ds-Rv	AGAGGAACTAGCCGGTGTT	51.1
CIP1-CDS-Fw	ATGAAAAAGCATAAGTTTAGAGAAACCTTG	52.5
CIP1-CDS-3U9-Rv	ACTGAGTCCTTAAGTTCGCTG	53.4
MAG2-CDS-Fw	ATGGAGGCGATCAAACCACTT	55.8
MAG2-CDS-Rv	CTAAGAGAACACTCTACTCTTCGCTAC	55.2
KAC1-CDS-Fw	ATGGCCGATCAGAGAAGTAAAACCAAT	56.2
KAC1-CDS-Rv	TTACTCCAGTTCACTAACAAGGTCCT	55.8
pHSBP-gBamHI-Fw	G<u>GGATCC</u>GACAAGCAGTTCCAGAGTTAAG	62.1
HSBP-ds-NcoI-Rv	TCT<u>CCATGG</u>CAGAGGAACTAGCCGGTGTTT	66.1
Point Mutations		
HSBP-R48K-Fw	ATGGGAGGCAAGATCAATGAG	56.1
HSBP-T17C-Rv	GACAAAAGCACACATATCAGC	53.2
HSBP-M16D/F19D-Rv	ATTTTGGACATCAGCAGTATCATCAGCAGT	61.0
HSBP-M16D/V20D-Rv	AAGATTTTGATCAAAAGCAGTATC	50.2
HSBP-I38R/I42R-Fw	ACTCCAGAATCACAAAGAGAGATGAC	56.4
HSBP-I42K/M45K-Fw	AAGAAGGATGACAAGGGAGGCAGAATCAATGAG	73.7

HSBP-I49K/L52K-Fw	AGAAAGAATGAGAAGGAGCAAAGCATCAATGAT	70.5
RT-PCR and qPCR		
MAG2-RT-Fw	CAGCACGATCCACAGGAAGT	53.8
MAG2-RT-Rv	TTCGGGTCTAACACACCACG	53.8
CIP1-RT-Fw	AAAGCGAGGAAGCCTCAGTG	53.8
CIP1-RT-Rv	TCTGCTTCGGTTTCGCTCTT	51.8
MAG2-qPCR-Fw	CGTGGTGTGTTAGACCCGAA	53.7
MAG2-qPCR-Rv	TCACGTAGCCACTTATCGCC	53.7
KAC1-qPCR-Fw	CTCTGGCCATGAAGGTTCCC	55.9
KAC1-qPCR-Rv	AGCATAACCAGCCAAAAATCTCA	51.7
CIP1-qPCR-Fw	GGTGTGCAAAAGCGAGGAAG	53.7
CIP1-qPCR-Rv	CTCGAGTTCTGCTCTCTGGC	55.8
CO-qPCR-Fw	TCGTGGCTGTTCCCTAATTC	56.5
CO-qPCR-Rv	GTACGCTGCAGTTTTGTTGG	56.2
CRY1-qPCR-Fw	CTGAACTGGAGACGGCTTTC	57.6
CRY1-qPCR-Rv	CAACCAGATTTCACCGGAGT	56.3
COP1-qPCR-Fw	TGTGGGTCTCACAGTGAACAGC	61.1
COP1-qPCR-Rv	CACGGGTCTCGTGATTTCCTTG	60.0
FT-qPCR-Fw	GCTACAACTGGAACAACCTTTGGC	60.7
FT-qPCR-Rv	ACTGTTTGCCTGCCAAGCTGTC	62.5
AP1-qPCR-Fw	TTGGCAAATGTTCGATGTTC	52.7
AP1-qPCR-Rv	TTCACGTTCATTCTCTCTGACC	55.9
HSP18.1-qPCR-Fw	GGATTCTTCACGCCATCTTCTG	57.7
HSP18.1-qPCR-Rv	ATGTGCCTCCGGCGTTT	59.4
HSFA1a-qPCR-Fw	AGCCCATTCCTTGATGGTGG	59.3
HSFA1a-qpCR-Rv	TCTCGGGGTCTTCGGGTATT	59.6
HSFA2-qpCR-Fw	GCAGCGTTGGATGTGAAAGTGG	61.2
HSFA2-qPCR-Rv	TTGGCTGTCCCAATCCAAAGGC	62.7
HSP101-qPCR-Fw	GGCGCTGGTGATCTTGTGTA	59.3

HSP101-qPCR-Rv	ATCTTCTTCACCGCCTGAGC	59.3
HSBP-qPCR-Fw	GTCGGACTCCATCATCACAAAG	57.2
HSBP-qPCR-Rv	CTTCTACTCCCATCTCGGCTCTTA	59.3
PP2AA3-Fw	CCTGCCGGTAATAACTGCATCT	58.6
PP2AA3-Rv	CTTCACTTAGCTCCACCAAGCA	58.7

Table 1. Primer sequence for genotyping, cloning, point mutations, RT-PCR and qPCR.

Restriction enzyme cutting sites were underlined as indicated.

Annotation	Locus	MW	pHSBP::HSBP-3xFLAG			35S::HSBP-3xFLAG		
			P	S	C	P	S	C
Normal Condition								
HSBP (Heat Shock Factor Binding Protein)	At4g15802	9kDa	7	21	74%	-	-	-
TGG2 (Glucoside glucohydrolase)	At5g25980	53.4kDa	4	4	14%	-	-	-
NDPK1 (Nucleoside diphosphate kinase family protein)	At4g09320	18.8kDa	2	2	15%	-	-	-
37 ℃ Heat Treatment for 1 hour								
HSBP, (Heat Shock Factor Binding Protein)	At4g15802	9kDa	7	22	74%	4	8	66%
ACT11, (Actin11)	At3g12110	42kDa	2	4	11%	-	-	-
TGG2, (Glucoside glucohydrolase)	At5g25980	53.4kDa	4	4	14%	-	-	-
ACT1, (Actin1)	At2g37620	42kDa	2	2	26%			
CIP1, (COP1-interactive protein1)	At5g41790	182kDa	-	-	-	59	87	46%
KAC1, Kinesin like protein for actin based chloroplast movement1	At5g10470	141kDa	-	-	-	33	43	39%
KAC2, Kinesin like protein for actin based chloroplast movement2	At5g65460	140kDa	-	-	-	17	18	26%
MAG2, Seed storage protein	At3g47700	90 kDa	-	-	-	9	10	19%
AtZW10, putative centromere/kinetochore protein	At2g32900	84 kDa	-	-	-	10	10	23%
Sec39, Secretory pathway 39	At5g24350	267 kDa	-	-	-	16	16	10%
Putative Sec-1 like domain-containing protein	At2g42700	92 kDa	-	-	-	5	5	8%
CSD1, Copper/Zinc superoxide dismutase 1	At1g08830	15 kDa	-	-	-	2	2	18%
MLP328, MLP-like protein 328	At2g01520	17 kDa	-	-	-	2	2	15%
Unknown Protein	At3g58110	90 kDa	-	-	-	9	12	17%

Table 2. LC-MS/MS result of AtHSBP interacting proteins.

This list was analyzed from LC-MS/MS data with in-solution digested of the HSBP co-immunoprecipitation samples from the *proHSBP::HSBP*-3xFLAG and *35S::HSBP*-3xFLAG 9-D-old plants under normal condition and 37 ℃ HS for 1 h. The *35S::*3xFLAG, as control, was used as non-specific/background for subtraction. Protein false discovery rate (FDR) and peptide FDR were both 0.00%, determined by Scaffold proteome software (version 4.3.2) at 99% threshold for protein identification and minimum of 2 peptides detected with 95% confidence. MW, molecular weight; P, exclusive unique peptides; S, exclusive unique spectra; C, percentage coverage. Data obtained from *35::*HSBP-3xFLAG was contributed by Chin-Cheng Liu.

Human	Arabidopsis	Results
L12D / V15D	M16D / F19D M16D / V20D	Break hexamer (trimer)
T13C	T17C	Stable hexamer (hexamer)
I34R / I38R	I38R / I42R	Break trimer (monomer)

| Maize	Arabidopsis	Results
R58K	R48K	Affect HSBP bind to HSF
I52K / M55K	I42K / M45K	Affect HSBP bind to HSF
I59K / L62K	I49K / L52K	Affect HSBP bind to HSF

Table 3. The structural alterations of mutated HSBP in human and maize and the corresponding mutation sites in Arabidopsis.
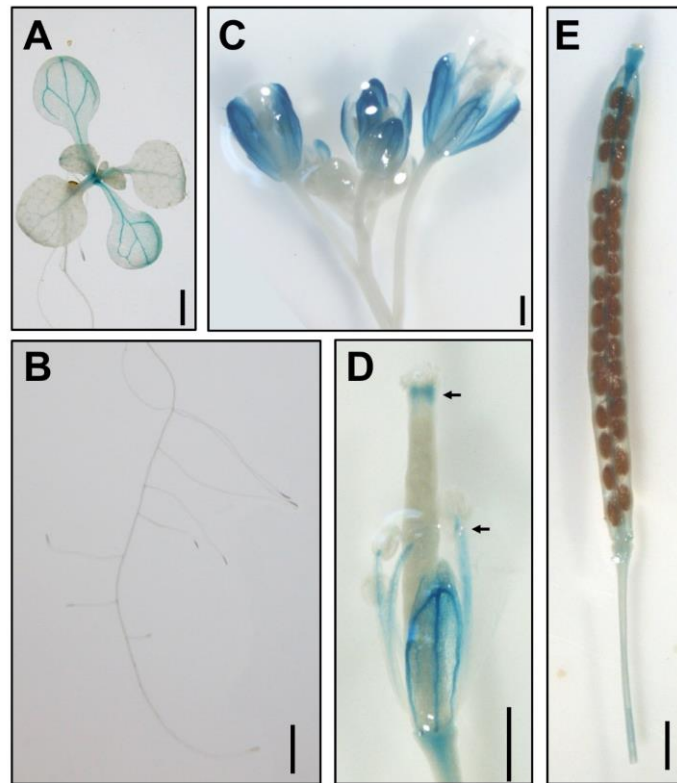
Figure 1. Spatial and temporal expression of *HSBP* by histochemical analysis.

Spatiotemporal expression pattern of the Arabidopsis HSBP in the transgenic plants of *proHSBP::GUS*. Promoter activity was visualized by histochemical GUS staining. (**A**) 12-d-old seedling, (**B**) 7-d-old root, (**C**) flowering bud cluster, (**D**) The closed-up view of flower and nascent silique, (**E**) silique tissue. GUS activity was observed in the seedlings leaves, petals, the anther filaments, the apex and base of nascent silique tissue and the valve and septum of mature silique. Arrows indicated the GUS activity in the nascent silique and in the anther filaments. The Scale bar = 1 mm.
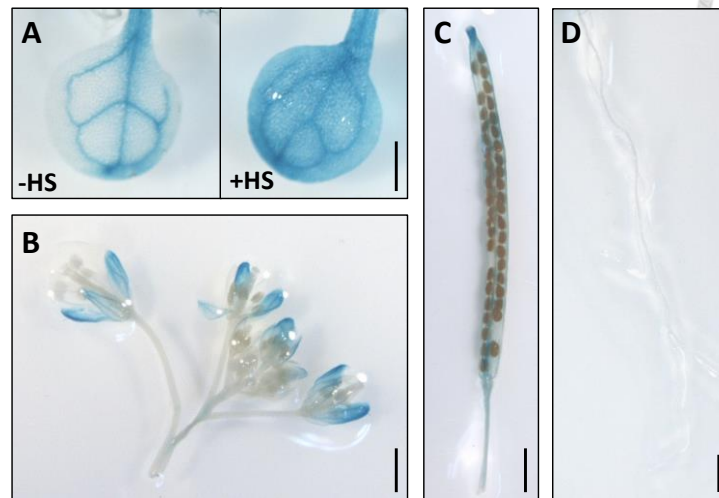
Figure 2. Spatial and temporal expression of *HSBP* after heat treatment.

(**A**) The cotyledons from the same seedling were trated without **(Left)** and with **(Right)**

a 37 °C HS for 1 h then the GUS activity was analyzed. (**B to D**) The expression of HSBP

on the flowering cluster, silique, and root showed no major differences after the HS as

indicated in **Figure 1**. Scale bar = 1mm
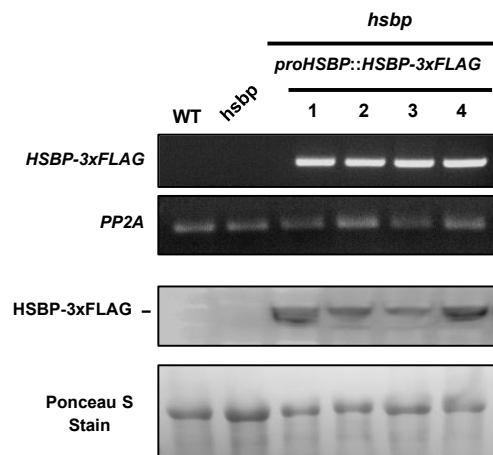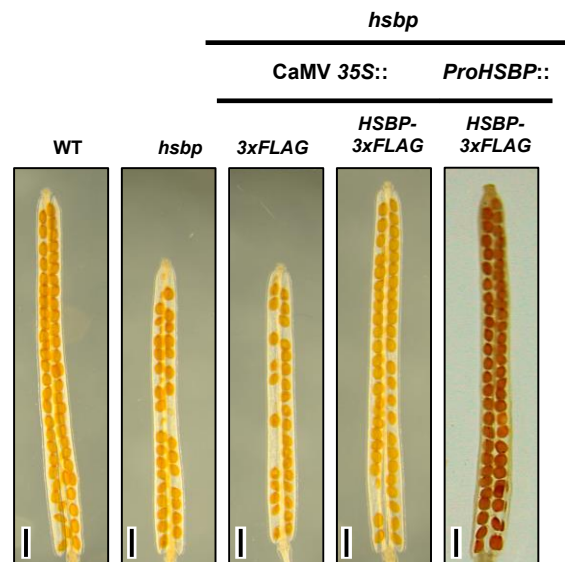
Figure 3. Characterization of *proHSBP::HSBP-3xFLAG* complementation line.

(**A**) The *HSBP* expression and protein level were confirmed by RT-PCR **(Upper)** and western blotting with α-FLAG antibodies **(Bottom)**. *PP2A* and Ponceau S staining were used as internal control for RT-PCR and western blotting, respectively. (**B**) Seed abortion and shorten silique phenotypes were rescued in *proHSBP::HSBP-3xFLAG* transgenic line compared to the *hsbp*.
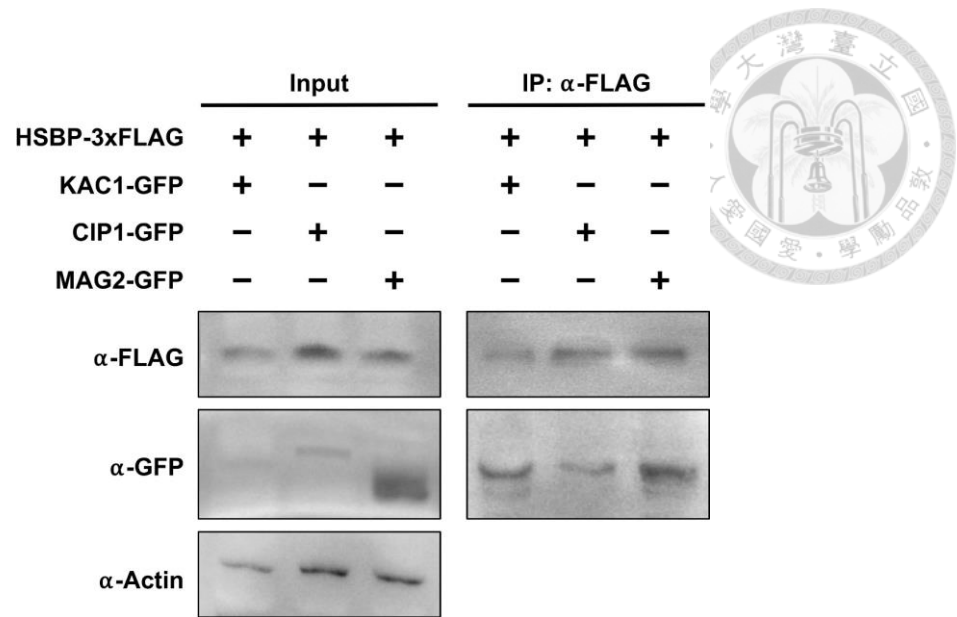
Figure 4. Co-immunoprecipitation (Co-IP) verification of the interaction between HSBP and HSBP-interacting proteins.

The protein-protein interaction of HSBP-3xFLAG with the GFP-tagged HSBP-interacting proteins KAC1, CIP1 and MAG2 were assessed by immunoprecipitation with the α-FLAG, and then western blotting was conducted by α-GFP antibodies. The MW of GFP-tagged KAC1, CIP1 and MAG2 is 167 kDa, 207 kDa and 117 kDa, respectively. Actin was used as a control.
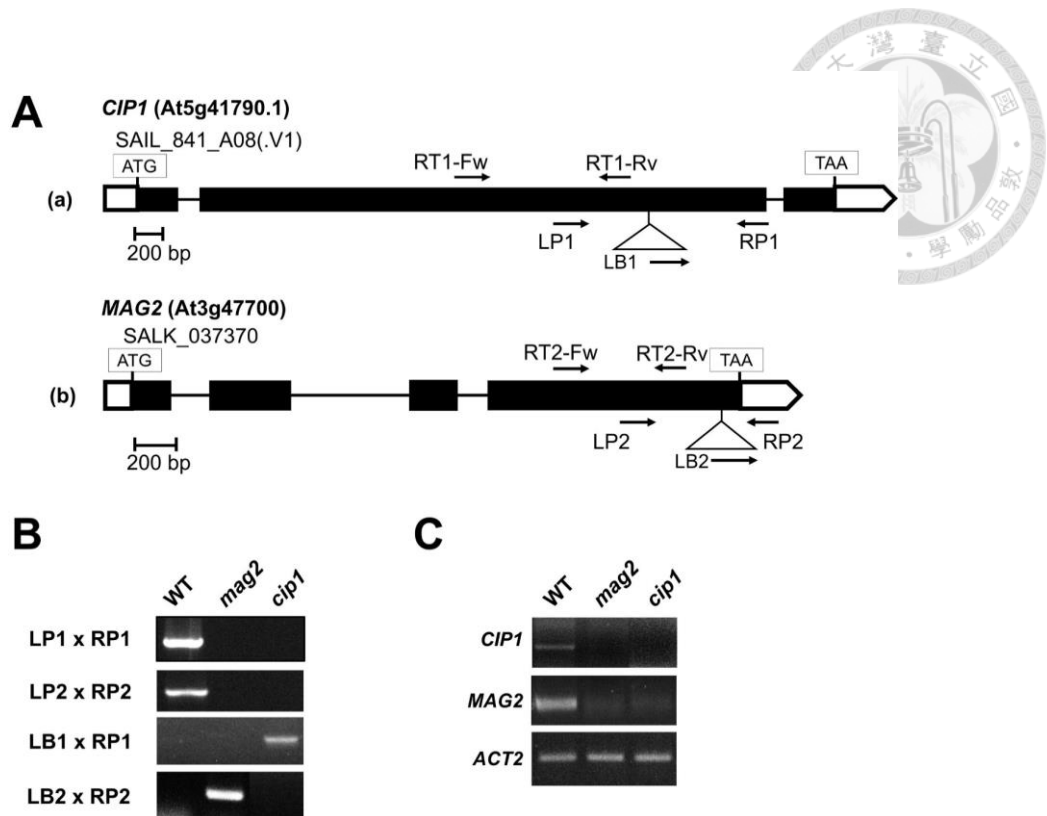
Figure 5. Identification and characterization of *cip1* and *mag2* T-DNA insertion line.

(**A**) Gene structure of CIP1 and MAG2 genomes are as indicated. Black boxes represents exons, lines indicate introns and white boxes are the UTR regions. The T-DNA insertion site of *cip1* mutant (SAIL_841_A08) locates at the second exon and the T-DNA insertion site of *mag2* (SALK_037370) locates at the fourth exon. (**B**) Genotyping of *cip1* and *mag2*. The PCR reaction with designed primer pairs, LPs xRPs and LBs x RPs. (**C**) RT-PCR results seggested that the *cip1* and *mag2* are null-mutant lines.
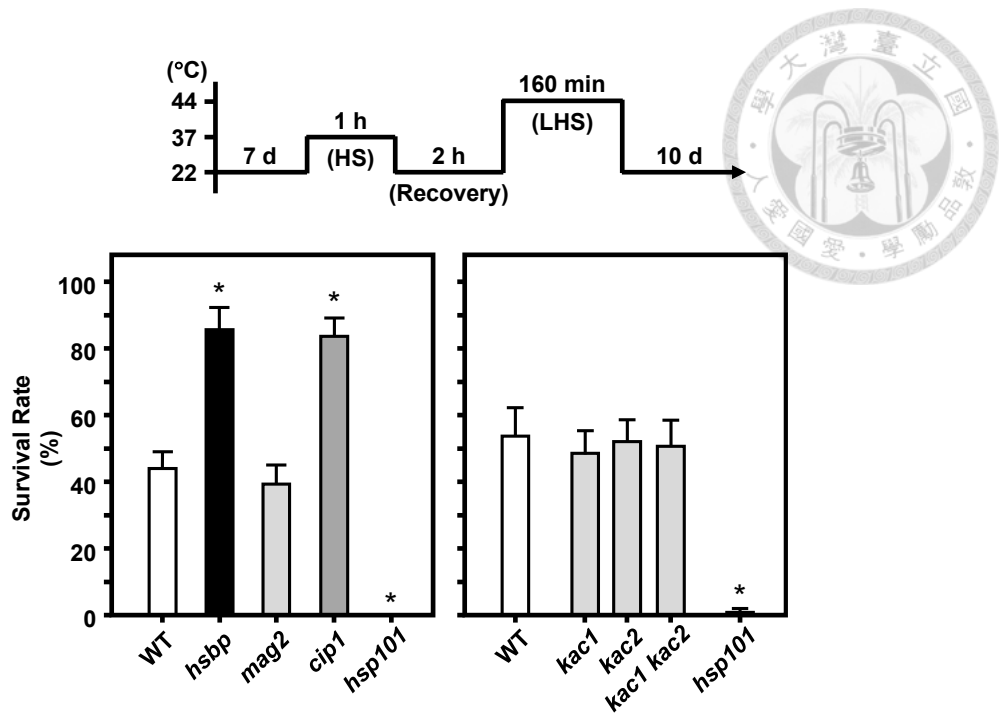
Figure 6. Acquired thermotolerance assay of mutants of HSBP interacting proteins.

Seven-d-old seedlings were treated with 37°C for 1 h and recovered at 22°C for 2 h, then subjected to 44°C lethal HS for 160 min, and the survival rate was determined 10 d after heat treatment. The *hsp101* mutant was used as a reference. Data are mean ± SD of 3 independent replicates (*n* = 50). *, Significance at *P* < 0.05 (Student's *t* test, as compared with the WT value).
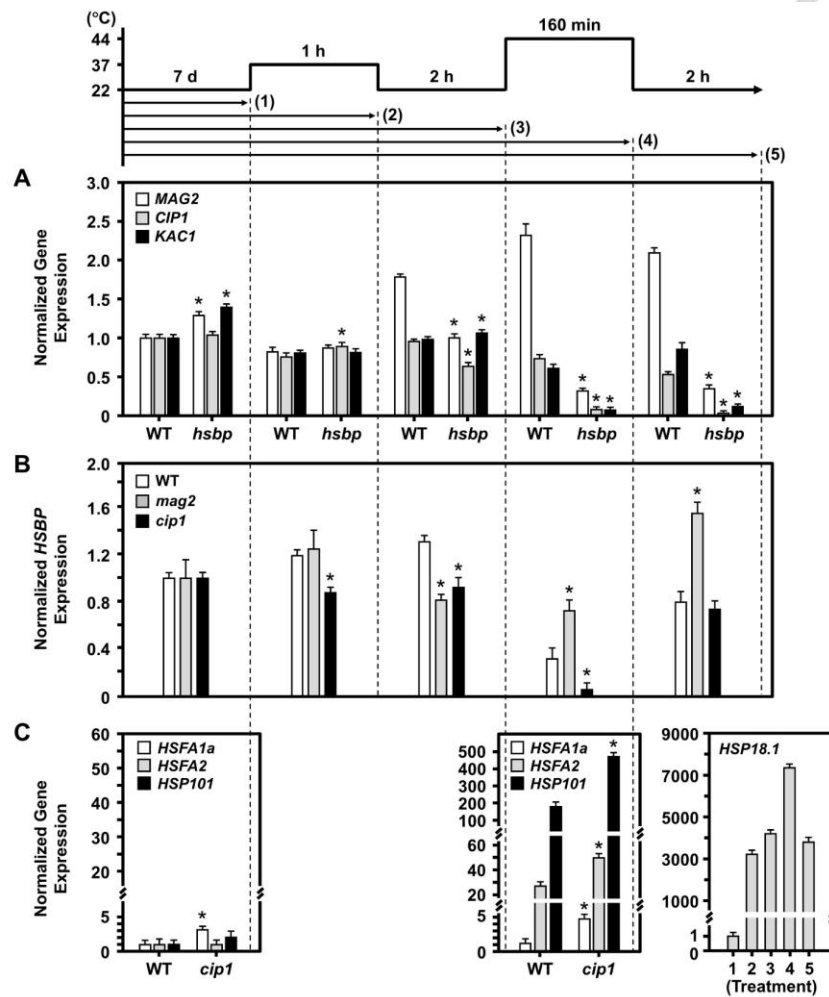
Figure 7. The expression level of *MAG2*, *CIP1* and *KAC1* and its mutants in response to heat.

The expression level of *HSBP*, *MAG2*, *CIP1*, and *KAC1* in response to HS was analyzed by qPCR in 7-day-old seedlings, as indicated. (**A**)The expression level of the tested gene in WT and *hsbp* mutant plants were analyzed. (**B**) The expression level of *HSBP* in *mag2* and *cip1* mutant plants were analyzed. (**C**) The expression level of HSR marker gene *HSFA1a*, *HSFA2* and *HSP101* in WT and *cip1* mutant plants were analyzed. Data are mean ± SD of 3 independent replicates (*n* = 9). *, Significance at *P* < 0.05 (Student's *t* test, as compared with the WT value).

77
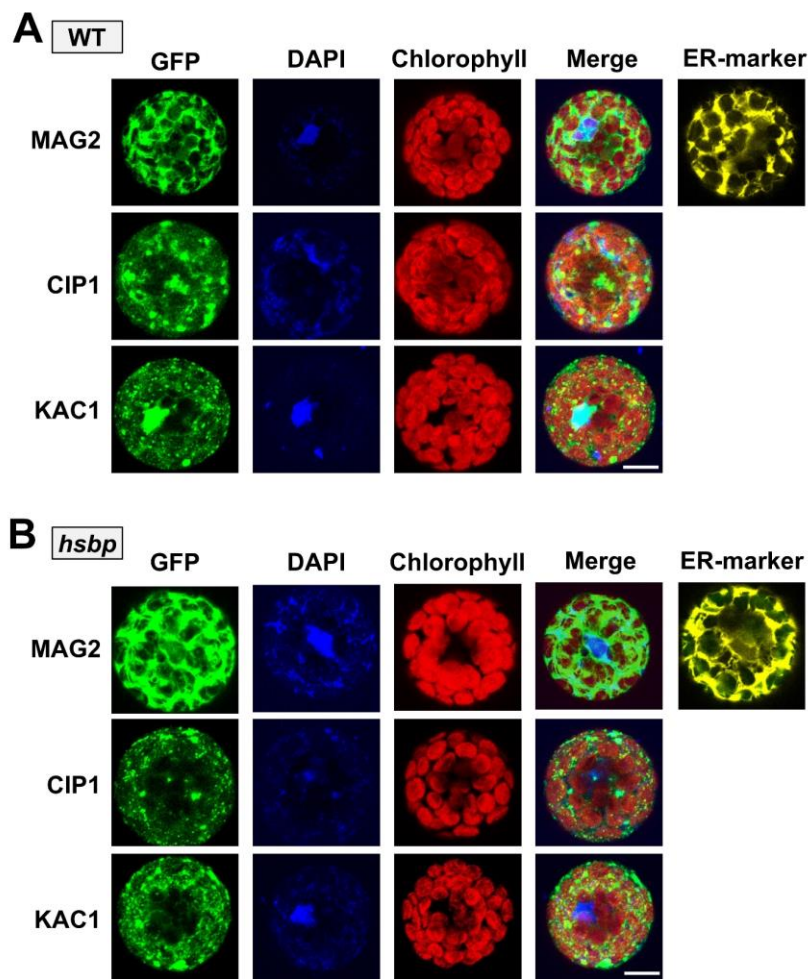
Figure 8. Subcellular localization of the HSBP-interacting proteins in WT and *hsbp* mutant protoplasts.

(A and B) GFP-tagged MAG2, CIP1, and KAC1 were analyzed in the WT or *hsbp* mutant protoplasts, respectively. The blue signal represents 4',6-diamidino-2-phenylindole (DAPI) stained nucleus with 359 nm of excitation and 461 nm of emission, the GFP signal was detected by 488 nm excitation and 505-530 nm of emission. The red signal indicates the auto fluorescence of chlorophyll. The ER-YFP obtained from ABRC is used as ER marker. Scale bar = 20 μm.
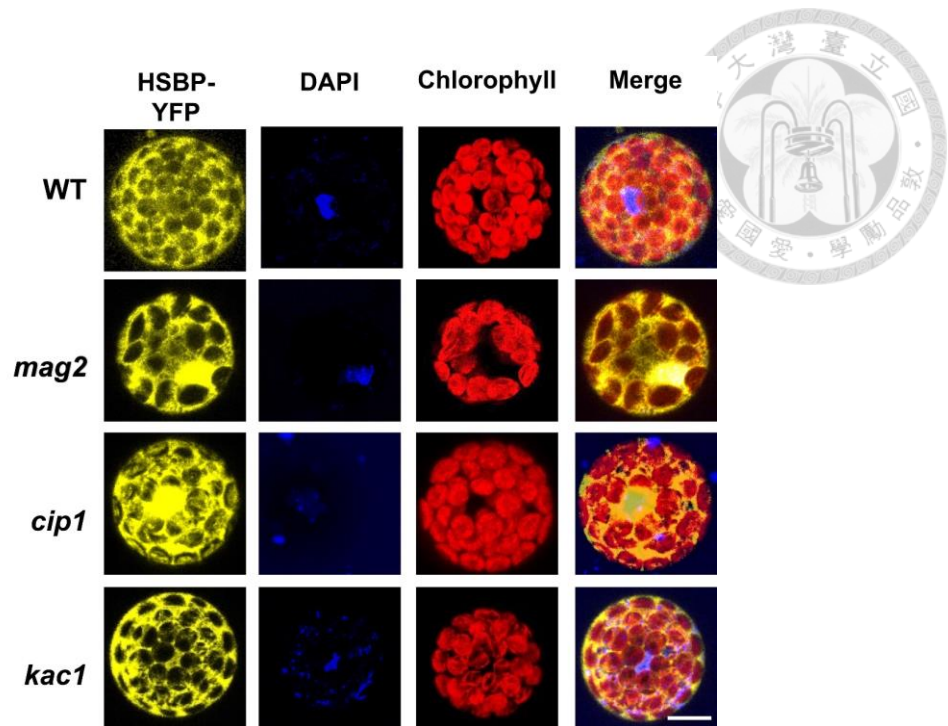
Figure 9. Subcellular localization of HSBP in *mag2*, *cip1* and *kac1* mutant protoplasts.

The HSBP-YFP was analyzed in the *mag2*, *cip1,* and *kac1* mutant protoplasts, as indicated

in **Figure 7**. The blue signal represents the DAPI stained nucleus. Scale bar = 20 μm.
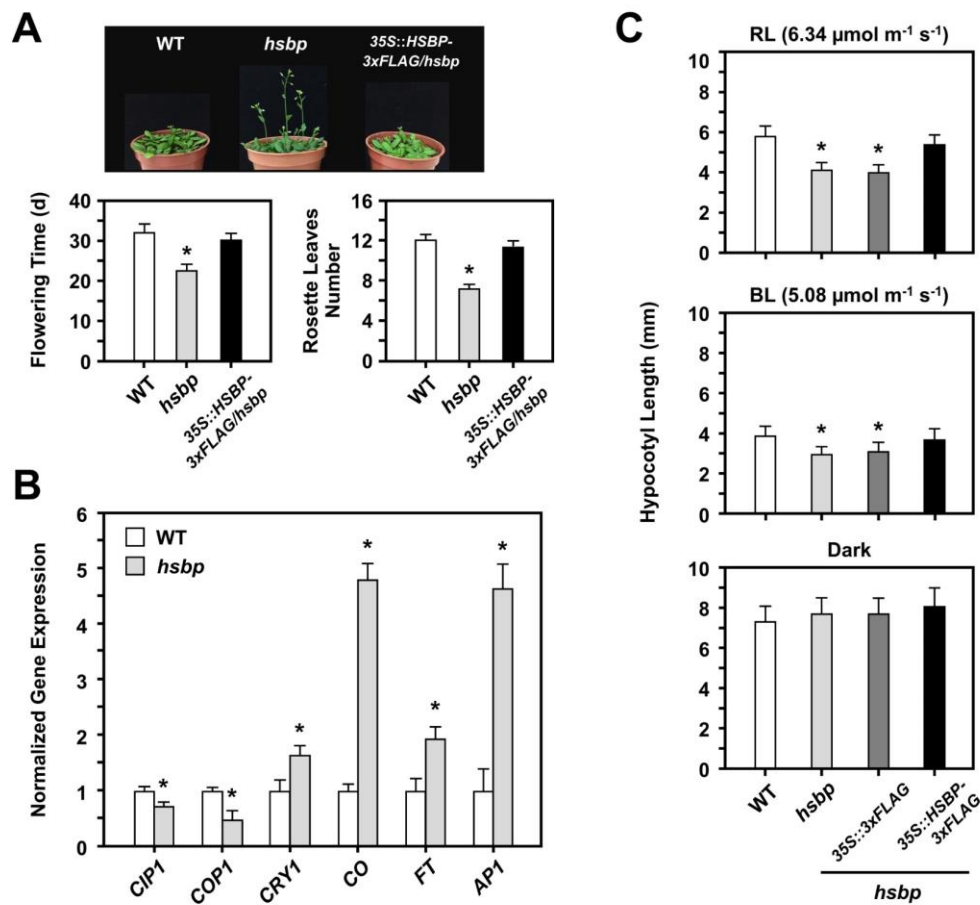
Figure 10. The effect of HSBP on flowering time and photomorphogenesis control.

(**A**) The photography of 30-d-old seedlings of the WT, *hsbp* mutant and transgenic plants overexpressing *HSBP-3xFLAG* in *hsbp* background. Flowering time (days) and rosette leave numbers when floral axis reaches 5 cm were measured. Data are mean ± SD of 3 independent replicates (*n* = 30). (**B**) 21-d-old seedlings were used for analysis of the flowering signal gene expression by qPCR. (**C**) Hypocotyl length was measured in 3-d-old seedlings grown under red light (RL, 6.34 μmol m^{-1} s^{-1}), blue light (BL, 5.08 μmol m^{-1} s^{-1}), and the dark. Data are mean ± SD of 3 independent replicates (*n* = 120). *, Significance at *P* < 0.05 (Student's *t* test, as compared with the WT value).
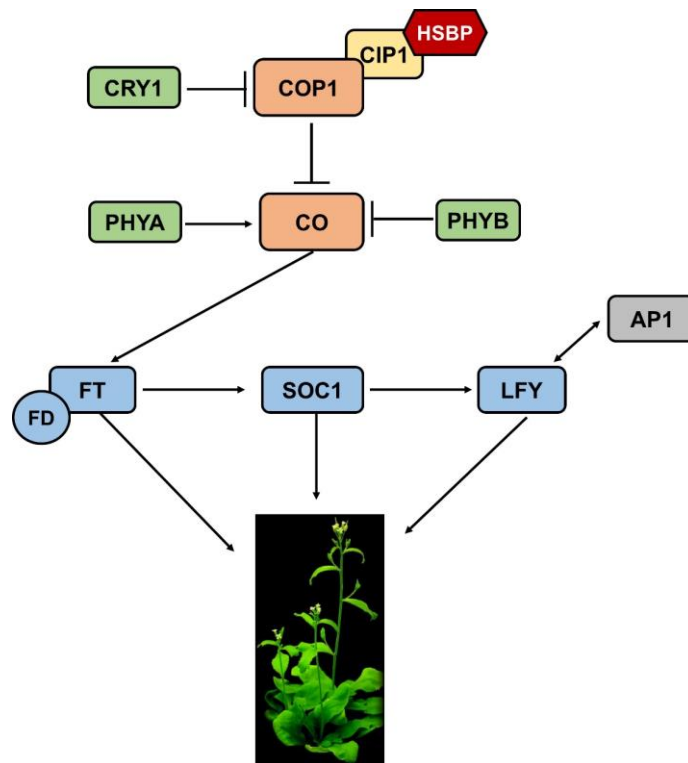
Figure 11. Proposed flowering signal transduction pathway.

A well-characterized flowering signal transduction pathway was highlighted. The *hsbp* mutant compared to the WT: the *COP1* and *CIP1* expression level were significantly downregulated, then *CO* expression level was upregulated; therefore, the downstream positive regulator of the *FT* and *AP1* expression level was upregulated to cause an early flowering phenotype. The *CRY1* expression was upregulated; thus, the higher expression level of *CO* was measured.
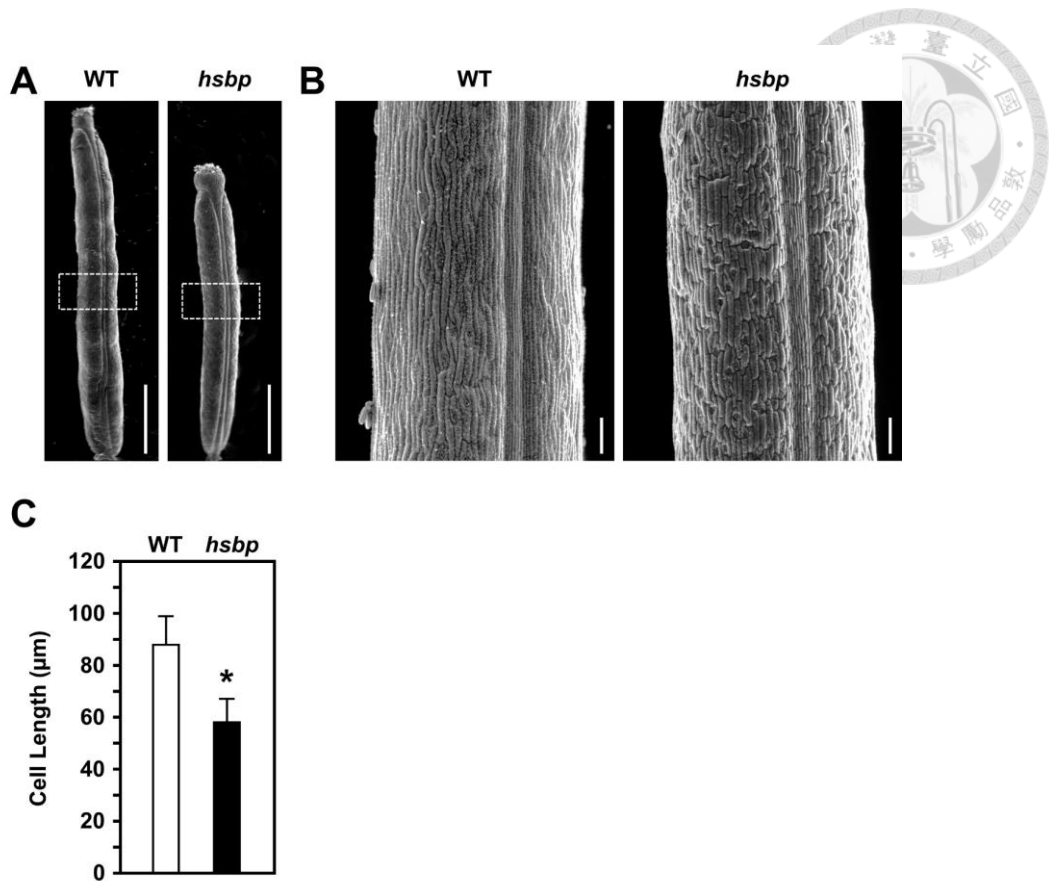
Figure 12. The silique cell length in _hsbp_ mutant.

(A) Scanning electron microscopy of green siliques of WT and _hsbp_ mutant at flower position 5. Bar = 1 mm. **(B)** Magnification of frames in panel A. Bars = 50 μm. **(C)** Measurement of carpel cell length in middle of siliques. Data are mean ± SD of 5 independent siliques ($n = 70$). *, Significance at $P < 0.05$ (Student's _t_ test, as compared with the WT value).
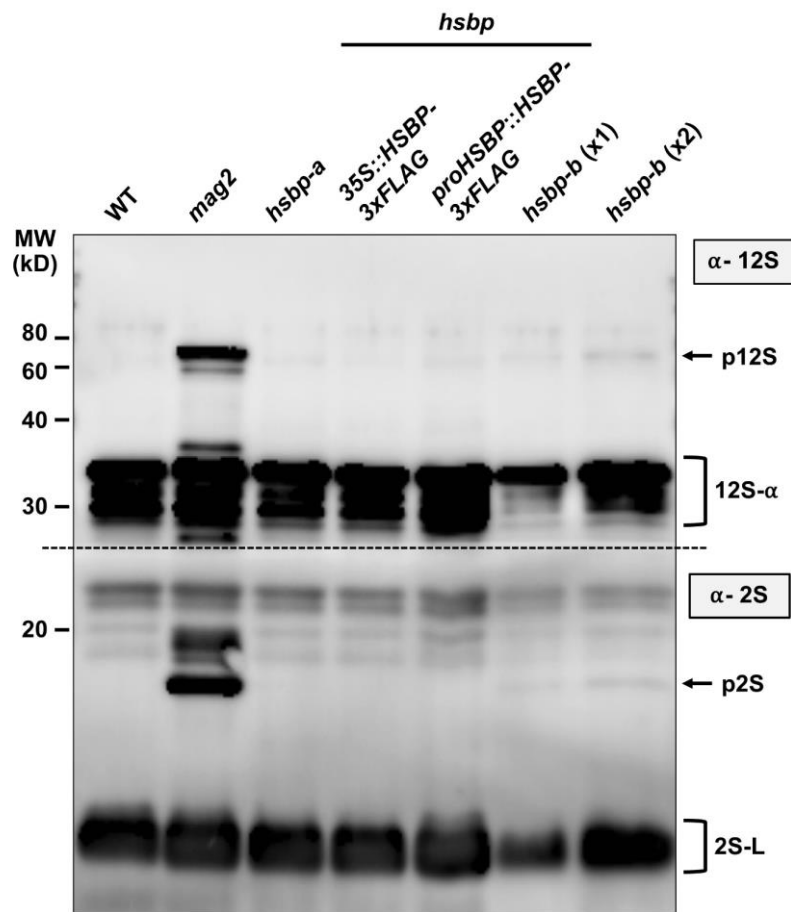
Figure 13. Analysis of the storage proteins of 12S globulins and 2S albumins.

Immunoblotting of dry seeds of the WT, *mag2*, *hsbp, and HSBP*-complementation (Comp)

and -overexpression (OE) in *hsbp* background with anti-12S globulin or anti-2S albumin

antibodies. The seeds of *hsbp-a* (phenotype similar to the WT), and *hsbp-b* (mild

phenotype) were collected from the siliques of *hsbp*. The *mag2* accumulated the

precursors, pro12S globulin (p12S) and pro2S albumin (p2S), as indicated by arrows. The

12S-a is 12S globulin subunit, and the 2S-L is 2S albumin subunits. Each lane contains

total proteins equivalent to one seed. The *hsbp-b* (x2) indicates a double volume. (by Dr.

Hara-Nishimura and Shimada)
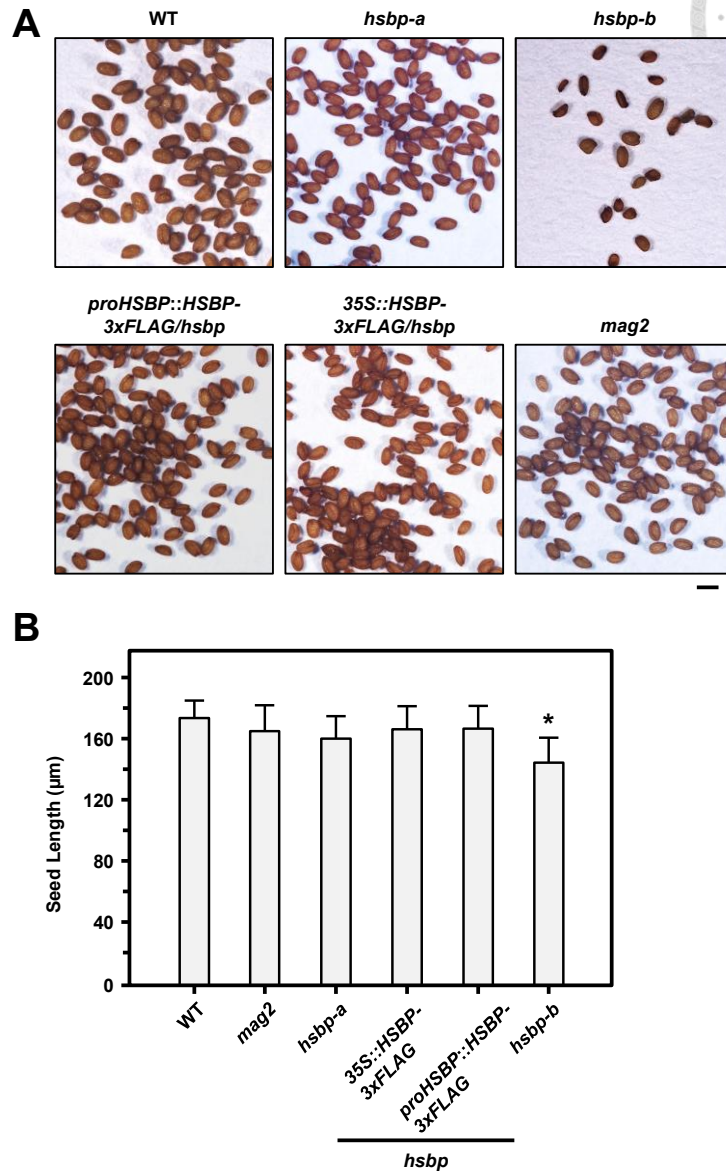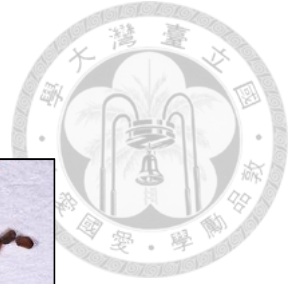
Figure 14. Seed phenotypes of WT, *mag2*, *hsbp,* and *HSBP*-complementation and -overexpression in *hsbp* mutant plants.

(A) The *hsbp* mutant plants showed two types of viable seeds (*hsbp-a* and *hsbp-b*). Bar = 200 μm. **(B)** Seed length measurement. $n > 20$. Data are mean ± SD (n > 20). *, Significance at $P < 0.05$ (Student's t test, as compared with the WT value).

84
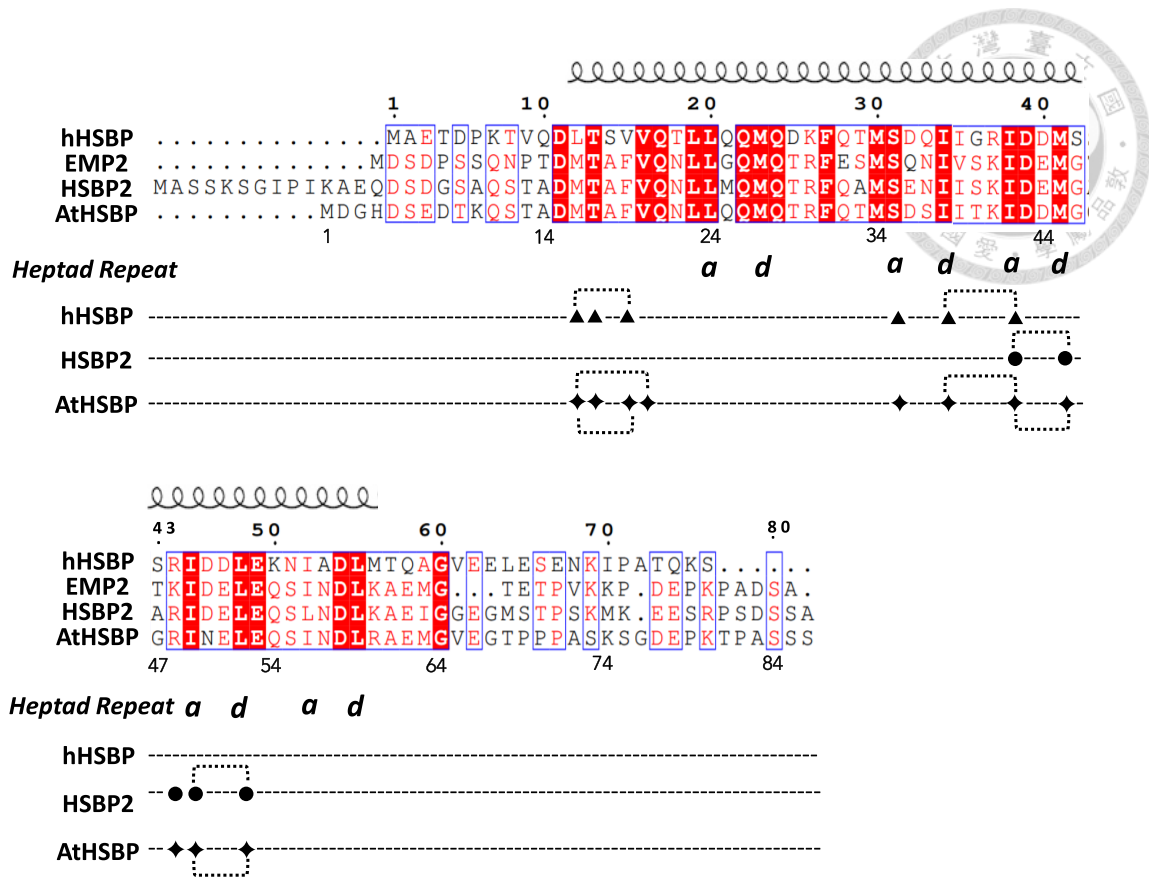
Figure 15. The HSBP homolog proteins sequence alignment and the sites for mutations.

The protein sequences of human HSBP (hHSBP), *Zea mays* EMP2 (HSBP2) and Arabidopsis HSBP (AtHSBP) was analyzed by CLUSTALW (version 2). The first and fourth residue of heptad repeat are indicated as "***a***" and "***d***". The corresponding mutation sites of hHSBP, HSBP2 and AtHSBP were labeled with ▲, ●, and ✦, respectively, as indicated. The "⋯" symbol represents the multiple mutations.
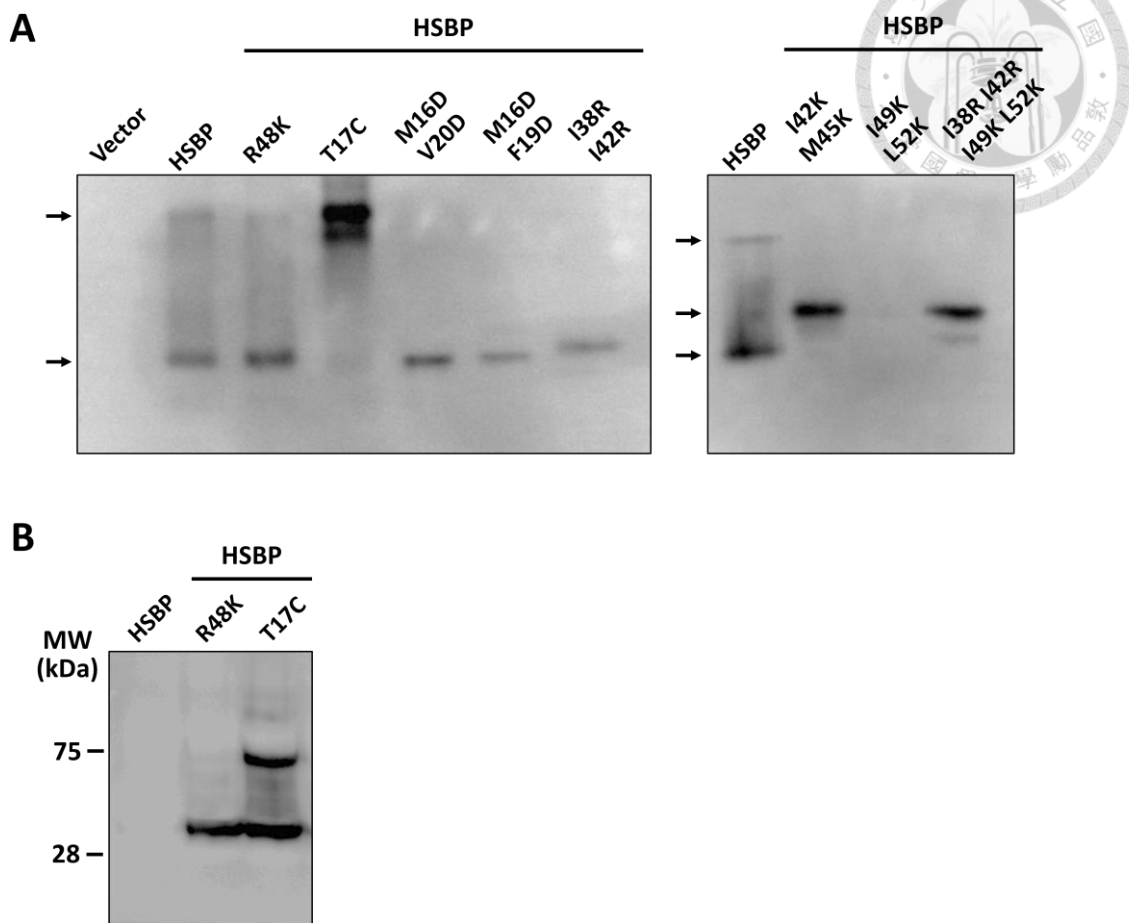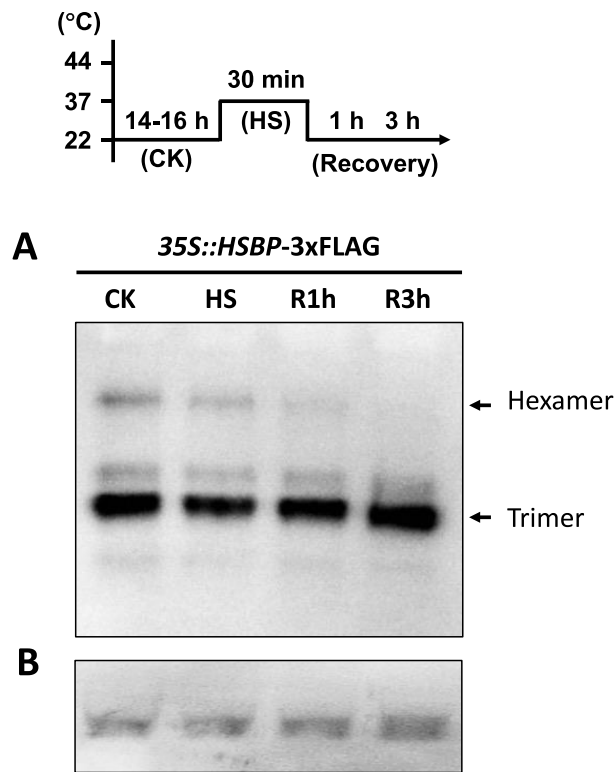
Figure 16. Oligomerization status of the Arabidopsis HSBP mutations.

(**A**) The oligomerization status of HSBP was analyzed by native-PAGE analyses. The HSBP

mutations were as indicated. (**B**) Samples did not subject to SDS and heat pretreatments

before spread in 12.5% SDS-PAGE.
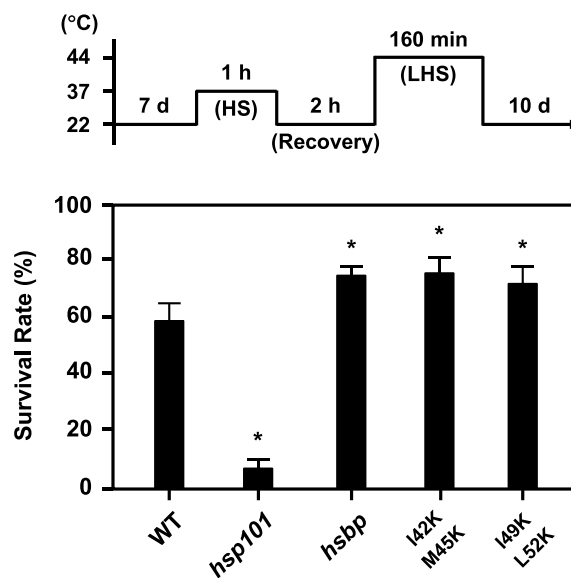
Figure 17. The HSBP mutation of I42K/M45K and I49K/L52K affacted the thermotolerance.

The transgenic lines of GFP fused HSBP-I42K/M45K and -I49K/L52K expressed in *hsbp* background was tested for acquired thermotolerance assay. The HS-sensitive *hsp101* mutant lants were used as controls. Data are mean ± SD of 3 independent replicates (*n* = 150). *, Significance at *P* < 0.05 (Student's *t* test, as compared with the WT value).

Figure 18. Oligomerization status of HSBP in response to HS.

WT protoplasts transformed with *35S::HSBP-3xFLAG* for 14 to 16 h then treated with cycloheximide for 2 h before the HS. The pictogram shows the HS regiem. (A and B) Native- and SDS-PAGE analyses of HSBP in response to HS, respectively. Arrows indicated the presumed hexamer and trimer form of HSBP, respectively.
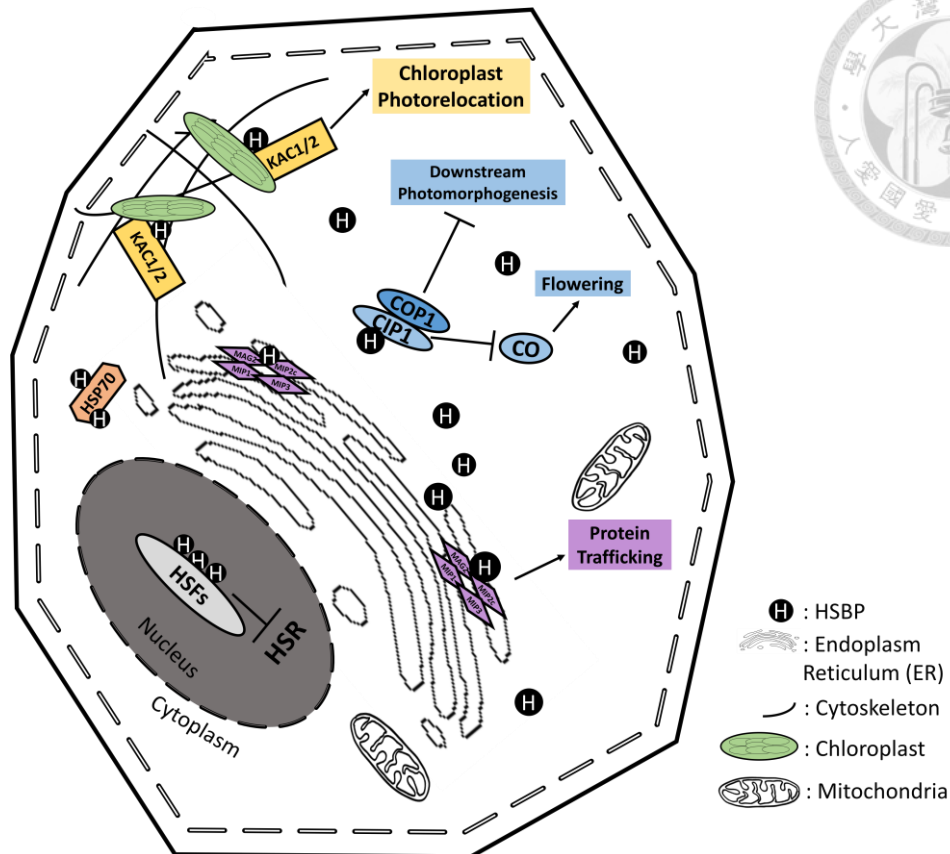
Figure 19. Illustration of HSBP functions in plant cells.

HSBP exists in both cytoplasm and nucleus to accomplish different functional roles. When heat stress occurs, HBSP assembles into trimer form and translocate to nucleus to attenuate the heat stress response by competing the binding site of heat shock elements with HSFs. In cytoplasm, HSBP has versatile functions. HSBP interacts with the MAG2 tethering complex on the ER and engages in the intracellular protein trafficking. The interaction between KAC1/2 and HSBP indicates that HBSP might be the novel member of the chloroplast cp-actin movement mediating complex. HSBP can also affects the light signal pathway by disturbing the stability of light signal center protein COP1 through interacting with CIP1 and influences the downstream photomorphogenesis and floweirng control.
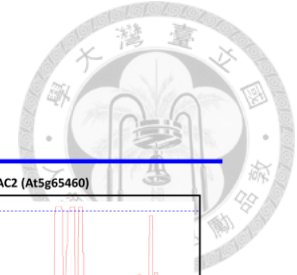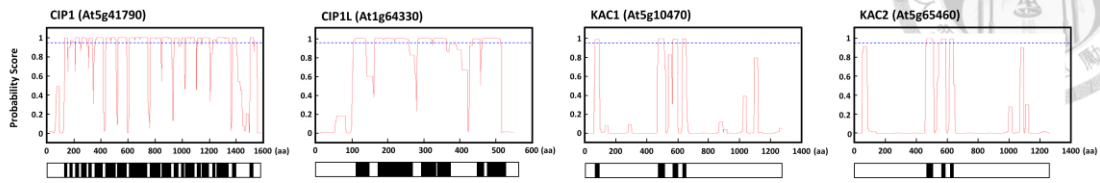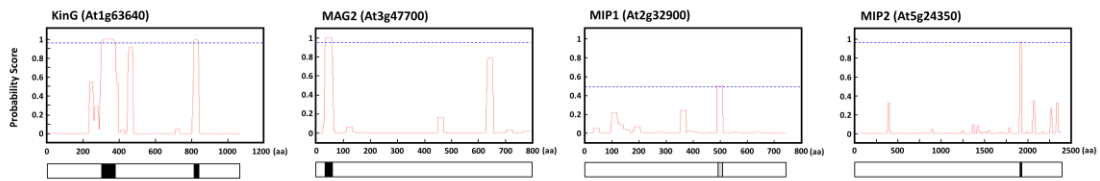
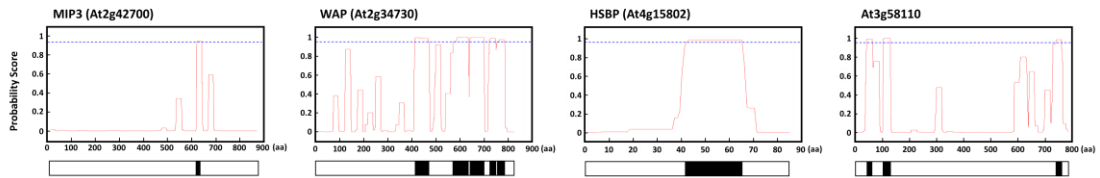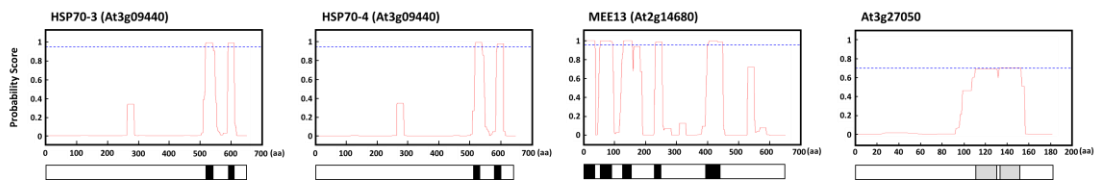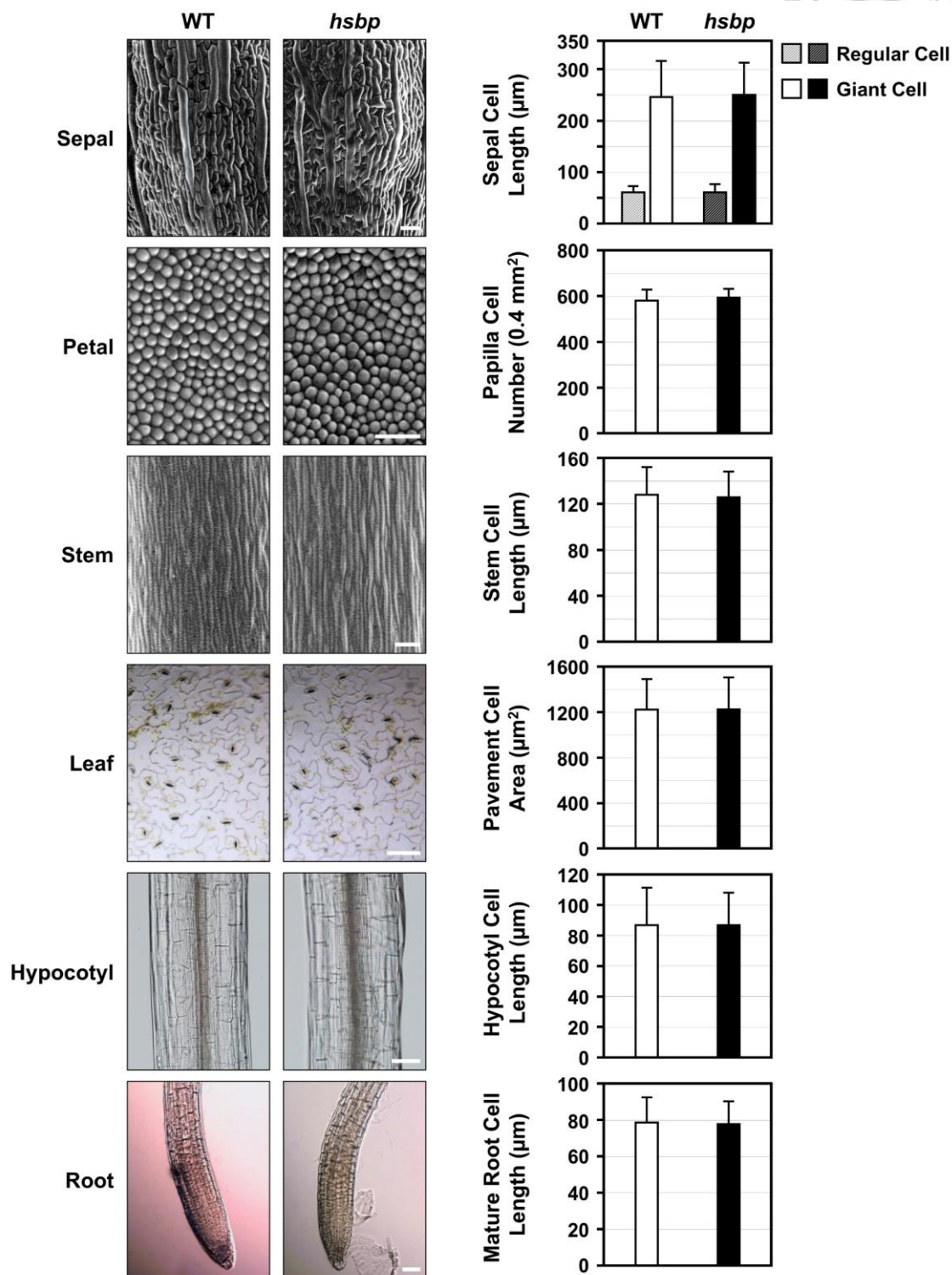**Appendix 1. Coiled-coil domain prediction of HSBP–interacting proteins.** The coiled-coil domains were predicted by the COILS program (http://www.ch.embnet.org/software/COILS_form.html; window of 21 residues). The coiled-coil domain prediction probability score cutoff > 95%, except for MIP1 and At3g27050, which is > 50% and 70%, respectively.

Appendix 2. Comparison of cell length in WT and *hsbp* plants. Cell phenotypes **(Left)**

and sizes were measured **(Right)** in WT and *hsbp* plants, as indicated.
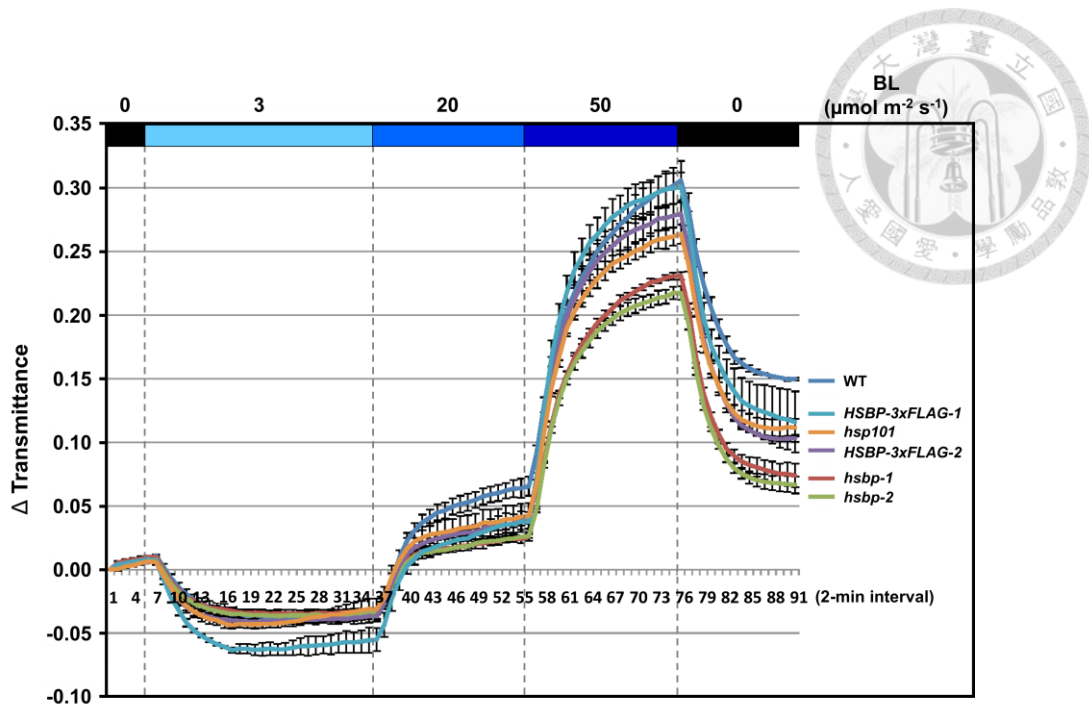
Appendix 3. Chloroplast photo-relocation movement assay in *hsbp* mutant. Red-light

transmittance in rosette leaves, increased and reduced under chloroplast avoidance and

accumulation response, respectively, was monitored under various blue light (BL)

intensities at 3, 20 and 50 μmol m^{-2} s^{-1} for the indicated times. The light-induced

transmittance changes were normalized to the transmission level of the starting point.

The transmittances were obtained from 4 to 8 leaves and were shown as a mean ± SD.

Two independent *hsbp*-mutant and *HSBP-3xFLAG*-complementation lines compared

with the WT were tested. The HS-sensitive mutant *hsp101* was a reference.
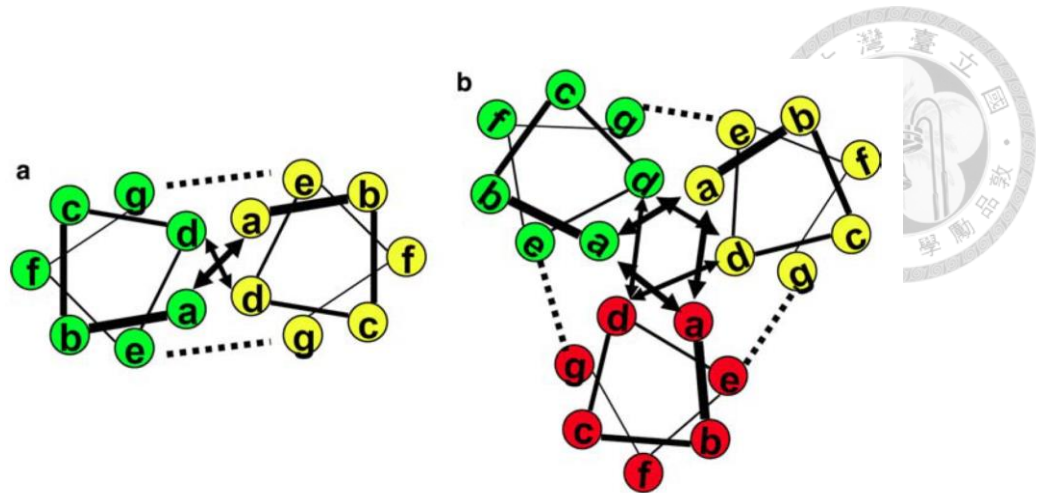
Appendix 4. Schematic illustration of coiled-coil domain structure and interactions.
Letters denote the seven amino acid residues ("***abcdefg***") comprising a hydrophobic heptad repeat. Hydrophobic and electrostatic interactions are designated by bidirectional arrows and dotted lines, respectively. (a) Helical wheel representation of a parallel two-stranded coiled coil, showing interactions between "***a***", "***d***", and "***e-g***" amino acid residues in the hydrophobic heptad repeats. (b) Helical wheel representation of hydrophobic and electrostatic interactions within a parallel three-stranded coiled-coil (Fu et al., 2006).
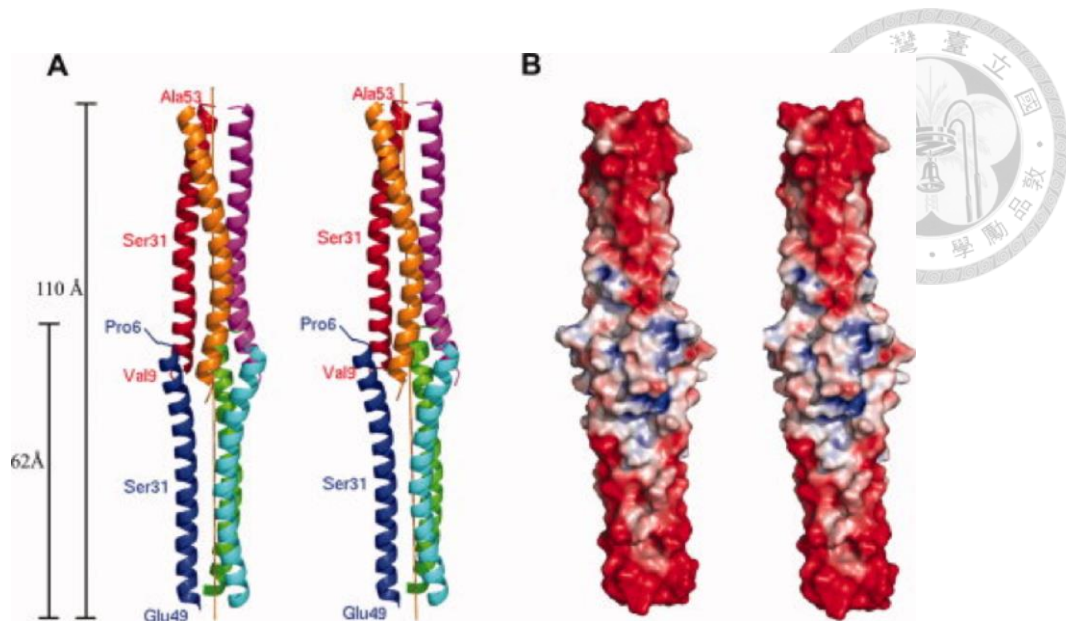
Appendix 5. Crystal structure of human HSBP1 hexamer structure. (A) Stereo view of the ribbon diagram of the hexamer structure. Each monomer is colored differently. The vertical line indicates the three-fold axis. The dimensions of the hexamer and trimer are labeled on the left. (B) Stereo view of HSBP1 hexamer surface electrostatic potential distribution. Electrostatic potential distribution was calculated with the program APBS. Positively charged regions (> +10 kT/e) are colored blue, and negatively charged regions (< -10 kT/e) in red. The picture was drawn with the program PyMol (http://www.pymol.org) (Liu et al., 2009).
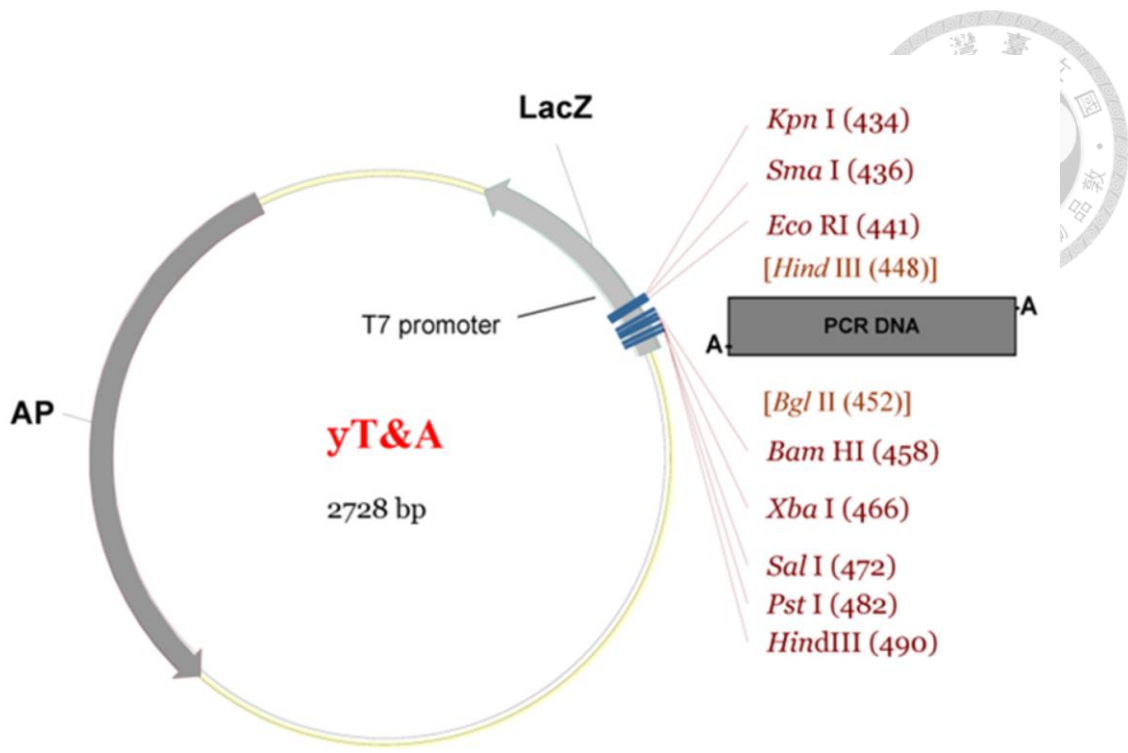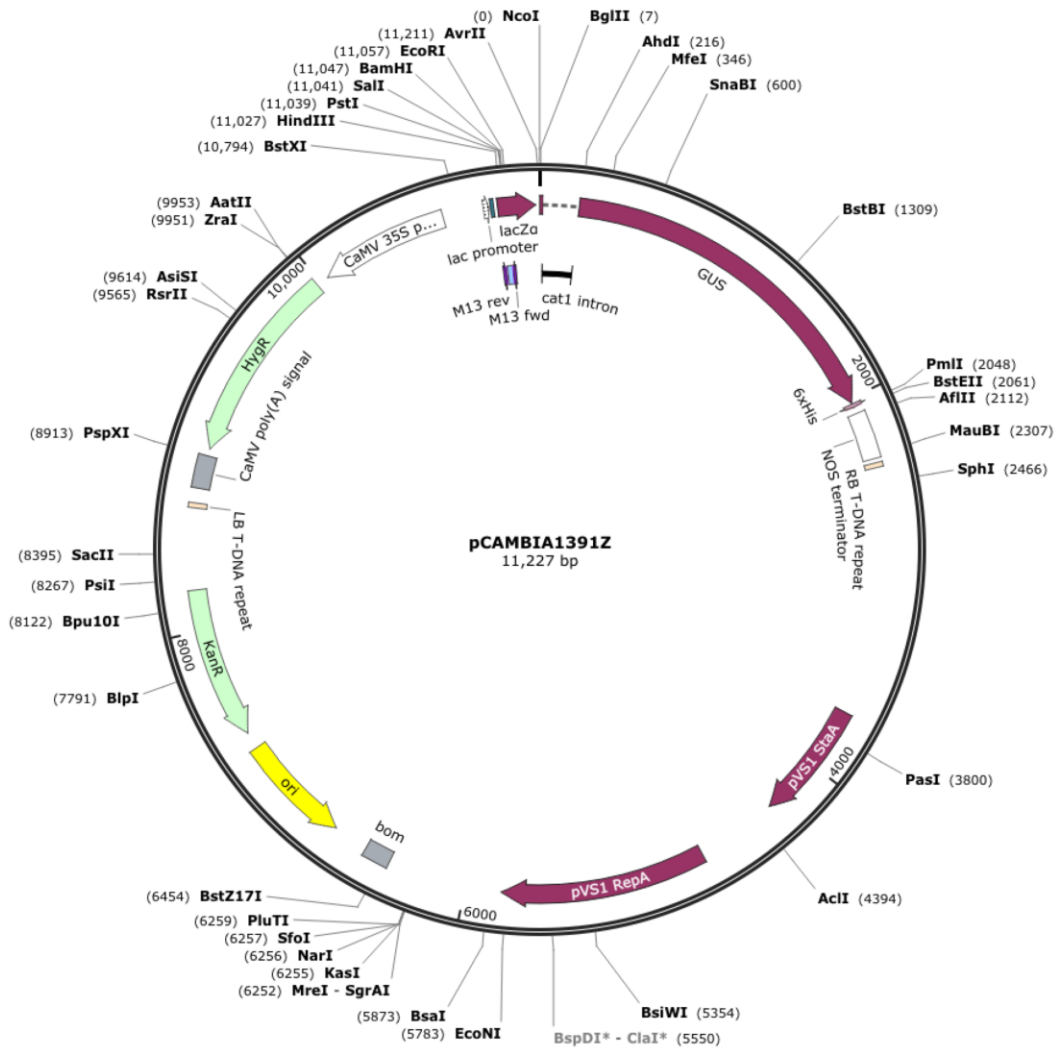
Appendix 6. The map of yT&A vector.
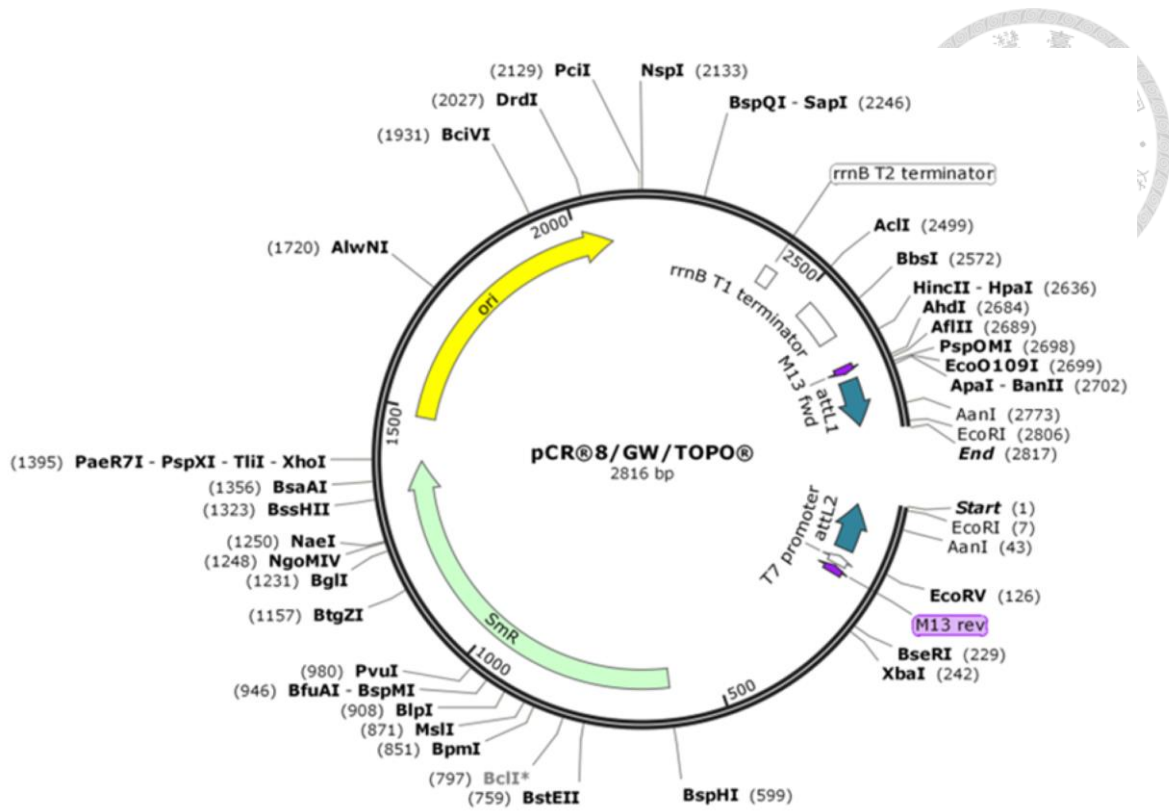
Appendix 7. The map of pCR8/GW/TOPO vector.

(0) **NcoI**
BglII (7)
(11,211) **AvrII**
AhdI (216)
(11,057) **EcoRI**
MfeI (346)
(11,047) **BamHI**
(11,041) **SalI**
SnaBI (600)
(11,039) **PstI**
(11,027) **HindIII**
(10,794) **BstXI**

BstBI (1309)

(9953) **AatII**
(9951) **ZraI**

CaMV 35S p...

lacZα
lac promoter

GUS

(9614) **AsiSI**
(9565) **RsrII**

M13 rev
M13 fwd
cat1 intron

10,000

HygR

6xHis

2000

PmlI (2048)
BstEII (2061)
AflII (2112)

(8913) **PspXI**

CaMV poly(A) signal

MauBI (2307)

RB T-DNA repeat
NOS terminator

SphI (2466)

LB T-DNA repeat

(8395) **SacII**
(8267) **PsiI**
(8122) **Bpu10I**

pCAMBIA1391Z
11,227 bp

KanR

(7791) **BlpI**

8000

ori

bom

PasI (3800)

4000

pVS1 StaA

AclI (4394)

pVS1 RepA

(6454) **BstZ17I**
(6259) **PluTI**
(6257) **SfoI**
(6256) **NarI**
(6255) **KasI**
(6252) **MreI - SgrAI**

6000

(5873) **BsaI**
(5783) **EcoNI**

BsiWI (5354)
BspDI* - ClaI* (5550)

Appendix 8. The map of pCAMBIA1391Z vector for generation of *proHSBP*::GUS transgenic line.

This plasmid contains *GUS* reporter gene downstream of multiple-cloning site (MCS; *Hind*III to *EcoR*I). The bacterial resistance marker is kanamycin, and the selection marker for Arabidopsis seedlings is hygromycin.
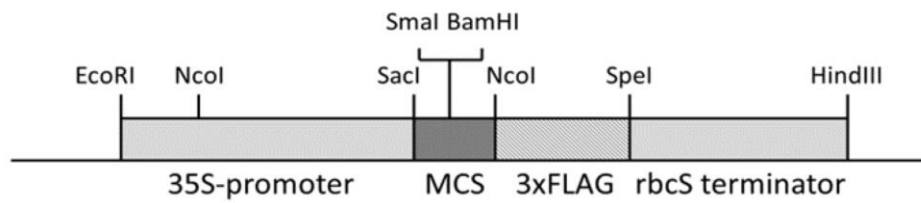
Appendix 9. The map of pCMABIA3300-CHF3-3xFLAG vector for generation of *proHSBP:*:HSBP-3xFLAG.

This plasmid contains CaMV *35S* promoter, and the 3xFLAG tag located at the C-terminal of multiple-cloning site (MCS). The bacterial resistance marker is kanamycin and the selection marker for Arabidopsis seedlings is BASTA.
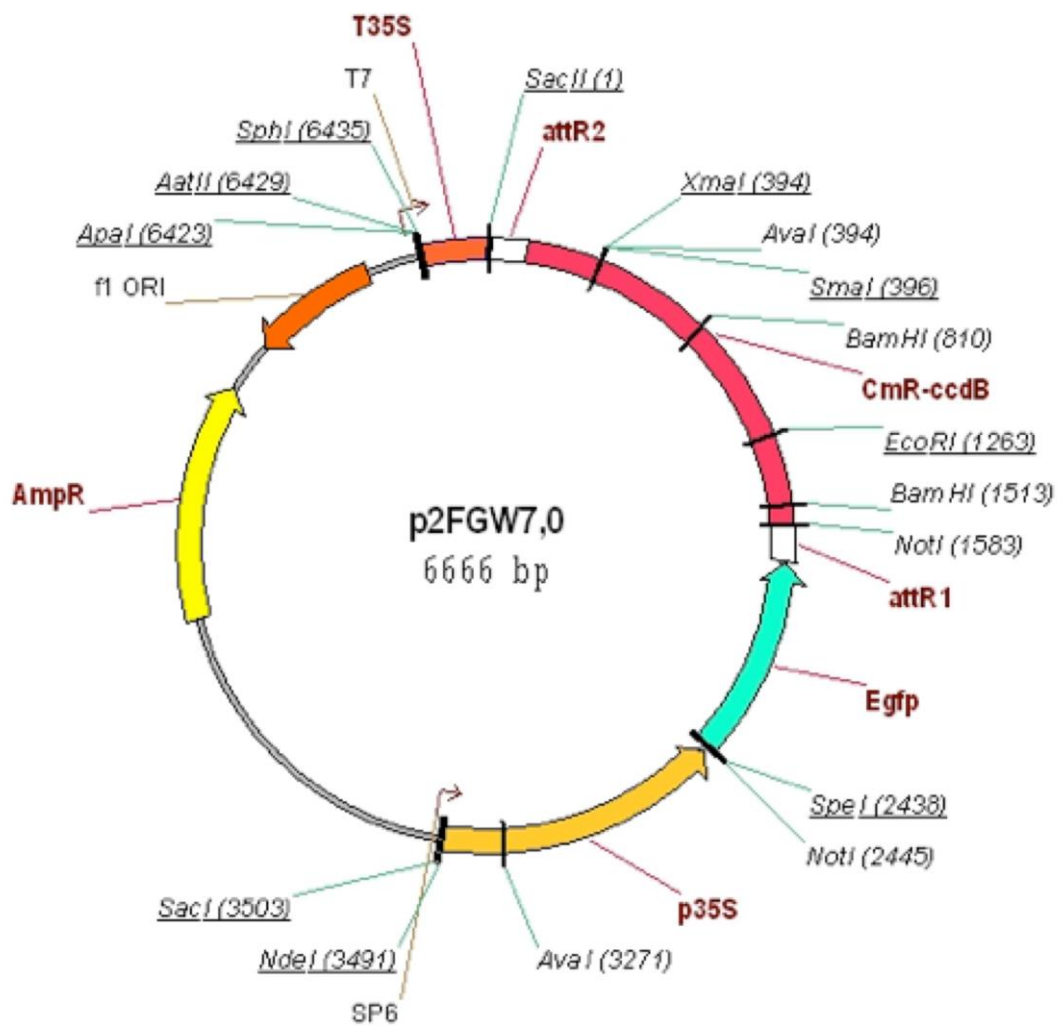
Appendix 10. The map of p2FGW7 vector.
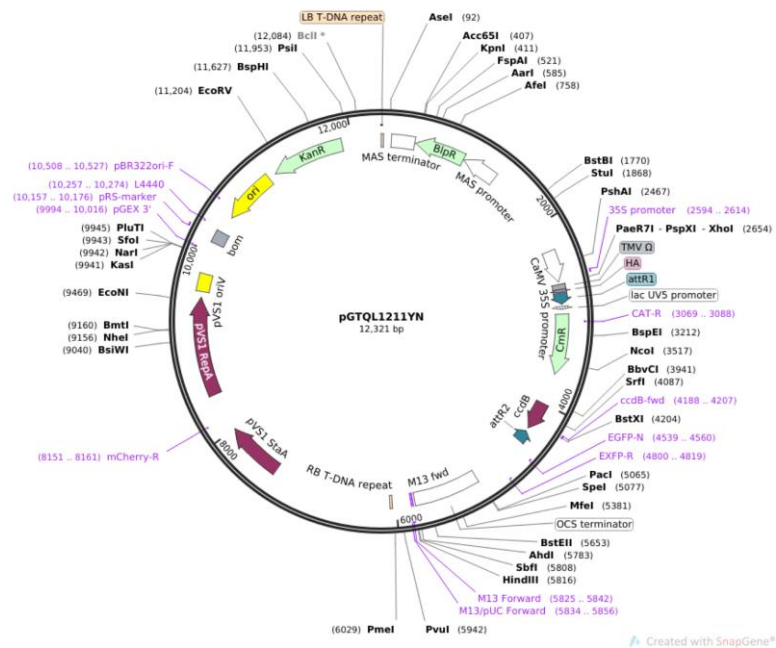
The vector is a gateway destination vector. The EGFP is located at the N-terminal of inserted site. The constructed plasmids are used for subcellular localization experiments. The bacterial resistance marker is kanamycin.

pGTQL1211YN
12,321 bp

pGTQL1221YC
12,028 bp
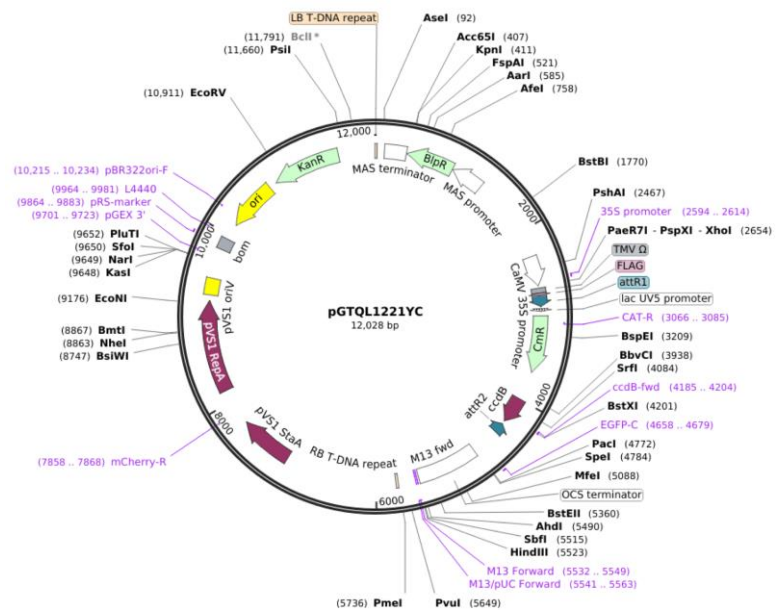
Appendix 11. The map of pGTQL1211YN (pEarleyGate201-YN) and pGTQL1221YC (pEarleyGate202-YC) vectors for BiFC experiments.
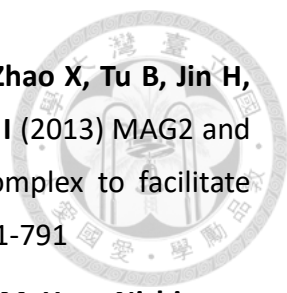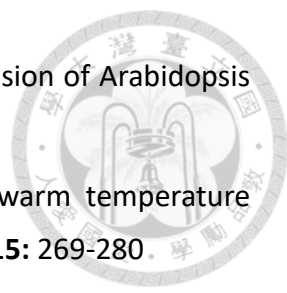
The vectors are gateway destination vectors. The N-terminal and C-terminal of YFP is located at the C-terminal of inserted site, respectively. The bacterial resistance marker is kanamycin.
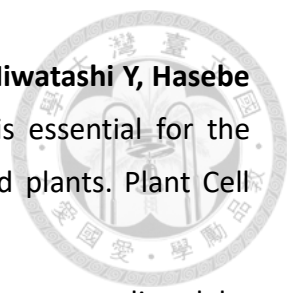
100

REFERENCES

Ahuja I, de Vos RC, Bones AM, Hall RD (2010) Plant molecular stress responses face climate change. Trends Plant Sci **15:** 664-674

Amasino RM, Michaels SD (2010) The timing of flowering. Plant Physiol **154:** 516-520

Barik S (2002) Megaprimer PCR. *In* B-Y Chen, HW Janes, eds, PCR cloning protocols. Humana Press, Totowa, NJ, pp 189-196

Baurle I, Dean C (2006) The timing of developmental transitions in plants. Cell **125:** 655-664

Bhattacharya J, Singh UK, Ranjan A (2017) Interaction of Light and Temperature Signaling at the Plant Interphase: From Cue to Stress. In: Senthil-Kumar M. (eds) Plant Tolerance to Individual and Concurrent Stresses. Springer, New Delhi

Bokszczanin KL, Fragkostefanakis S (2013) Perspectives on deciphering mechanisms underlying plant heat stress response and thermotolerance. Front Plant Sci **4:** 315

Ciani B, Bjelic S, Honnappa S, Jawhari H, Jaussi R, Payapilly A, Jowitt T, Steinmetz MO, Kammerer RA (2010) Molecular basis of coiled-coil oligomerization-state specificity. Proc Natl Acad Sci U S A **107:** 19850-19855

Clough SJ, Bent AF (1998) Floral dip: a simplified method for Agrobacterium-mediated transformation of *Arabidopsis thaliana*. Plant J **16:** 735-743

Eroglu B, Min J-N, Zhang Y, Szurek E, Moskophidis D, Eroglu A, Mivechi NF (2014) An essential role for heat shock transcription factor binding protein 1 (HSBP1) during early embryonic development. Dev Biol **386:** 448-460

Fornara F, de Montaigu A, Coupland G (2010) SnapShot: control of flowering in Arabidopsis. Cell **141:** 550, 550.e551-552

Franklin KA, Toledo-Ortiz G, Pyott DE, Halliday KJ (2014) Interaction of light and temperature signalling. J Exp Bot **65:** 2859-2871

Fu S, Meeley R, Scanlon MJ (2002) Empty pericarp2 encodes a negative regulator of the heat shock response and is required for maize embryogenesis. Plant Cell **14:** 3119-3132

Fu S, Rogowsky P, Nover L, Scanlon MJ (2006) The maize heat shock factor-binding protein paralogs EMP2 and HSBP2 interact non-redundantly with specific heat shock factors. Planta **224:** 42-52
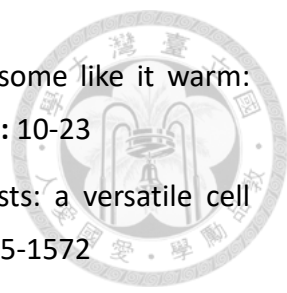
Fu S, Scanlon MJ (2004) Clonal mosaic analysis of EMPTY PERICARP2 reveals nonredundant functions of the duplicated HEAT SHOCK FACTOR BINDING PROTEINs during maize shoot development. Genetics **167:** 1381-1394

Fujiwara T, Nambara E, Yamagishi K, Goto DB, Naito S (2002) Storage Proteins. The Arabidopsis Book**:** e0020

Golembeski GS, Imaizumi T (2015) Photoperiodic Regulation of Florigen Function in *Arabidopsis thaliana*. Arabidopsis Book **13:** e0178

Guo M, Liu JH, Ma X, Luo DX, Gong ZH, Lu MH (2016) The Plant Heat Stress Transcription factors (HSFs): structure, regulation, and Function in Response to Abiotic Stresses. Front Plant Sci **7:** 114

Heath JD, Weldon R, Monnot C, Meinke DW (1986) Analysis of storage proteins in normal and aborted seeds from embryo-lethal mutants of *Arabidopsis thaliana*. **v. 169:** 304-312

Hsu SF, Jinn TL (2010) AtHSBP functions in seed development and the motif is required for subcellular localization and interaction with AtHSFs. Plant Signal Behav **5:** 1042-1044

Hsu SF, Lai HC, Jinn TL (2010) Cytosol-localized heat shock factor-binding protein, AtHSBP, functions as a negative regulator of heat shock response by translocation to the nucleus and is required for seed development in Arabidopsis. Plant Physiol **153:** 773-784

Jang K, Lee HG, Jung SJ, Paek NC, Seo PJ (2015) The E3 ubiquitin ligase COP1 Regulates thermosensory flowering by triggering GI degradation in Arabidopsis. Sci Rep **5:** 12071

Kodama Y, Suetsugu N, Kong SG, Wada M (2010) Two interacting coiled-coil proteins, WEB1 and PMI2, maintain the chloroplast photorelocation movement velocity in Arabidopsis. Proc Natl Acad Sci U S A **107:** 19591-19596

Kotak S, Larkindale J, Lee U, von Koskull-Doring P, Vierling E, Scharf KD (2007) Complexity of the heat stress response in plants. Curr Opin Plant Biol **10:** 310-316

Lau OS, Deng XW (2012) The photomorphogenic repressors COP1 and DET1: 20 years later. Trends Plant Sci **17:** 584-593

Li L, Shimada T, Takahashi H, Koumoto Y, Shirakawa M, Takagi J, Zhao X, Tu B, Jin H, Shen Z, Han B, Jia M, Kondo M, Nishimura M, Hara-Nishimura I (2013) MAG2 and three MAG2-INTERACTING PROTEINs form an ER-localized complex to facilitate storage protein transport in *Arabidopsis thaliana*. Plant J **76**: 781-791

Li L, Shimada T, Takahashi H, Ueda H, Fukao Y, Kondo M, Nishimura M, Hara-Nishimura I (2006) MAIGO2 is involved in exit of seed storage proteins from the endoplasmic reticulum in *Arabidopsis thaliana*. Plant Cell **18**: 3535-3547

Liu CC, Jinn TL (2014) Interactomic Profile of MicroProtein-like Heat Shock Factor Binding Protein, a Negative Regulator of Heat Shock Response, Under Heat Stress and Recovery Stages. (Master Thesis)

Liu LJ, Zhang YC, Li QH, Sang Y, Mao J, Lian HL, Wang L, Yang HQ (2008) COP1-mediated ubiquitination of CONSTANS is implicated in cryptochrome regulation of flowering in Arabidopsis. Plant Cell **20:** 292-306

Liu X, Xu L, Liu Y, Tong X, Zhu G, Zhang XC, Li X, Rao Z (2009) Crystal structure of the hexamer of human heat shock factor binding protein 1. Proteins **75**: 1-11

Machettira A, Groß L, Tillmann B, Weis B, Englich G, Sommer M, Königer M, Schleiff E (2012) Protein-induced modulation of chloroplast membrane morphology. Front Plant Sci **2**: 1-11

Mason JM, Arndt KM (2004) Coiled coil domains: stability, specificity, and biological implications. Chembiochem **5**: 170-176

Matsui M, Stoop CD, von Arnim AG, Wei N, Deng XW (1995) Arabidopsis COP1 protein specifically interacts in vitro with a cytoskeleton-associated protein, CIP1. Proc Natl Acad Sci U S A **92**: 4239-4243

Mayer MP, Bukau B (2005) Hsp70 chaperones: cellular functions and molecular mechanism. Cell Mol Life Sci **62**: 670-684

Mittler R, Finka A, Goloubinoff P (2012) How do plants feel the heat? Trends Biochem Sci **37**: 118-125

Mylne JS, Hara-Nishimura I, Rosengren KJ (2014) Seed storage albumins: biosynthesis, trafficking and structures. Funct Plant Biol **41**: 671-677

Nover L, Bharti K, Doring P, Mishra SK, Ganguli A, Scharf KD (2001) Arabidopsis and the heat stress transcription factor world: how many heat stress transcription factors do we need? Cell Stress Chaperones **6**: 177-189

Osterlund MT, Ang LH, Deng XW (1999) The role of COP1 in repression of Arabidopsis photomorphogenic development. Trends Cell Biol **9:** 113-118

Park YJ, Lee HJ, Ha JH, Kim JY, Park CM (2017) COP1 conveys warm temperature information to hypocotyl thermomorphogenesis. New Phytol **215:** 269-280

Qin F, Shinozaki K, Yamaguchi-Shinozaki K (2011) Achievements and challenges in understanding plant abiotic stress responses and tolerance. Plant Cell Physiol **52:** 1569-1582

Rana RM, Dong S, Tang H, Ahmad F, Zhang H (2012) Functional analysis of OsHSBP1 and OsHSBP2 revealed their involvement in the heat shock response in rice (*Oryza sativa L.*). J Exp Bot **63:** 6003-6016

Ren C, Zhu X, Zhang P, Gong Q (2016) Arabidopsis COP1-interacting protein 1 is a positive regulator of ABA response. Biochem Biophys Res Commun **477:** 847-853

Richter K, Haslbeck M, Buchner J (2010) The heat shock response: life on the verge of death. Mol Cell **40:** 253-266

Satyal SH, Chen D, Fox SG, Kramer JM, Morimoto RI (1998) Negative regulation of the heat shock transcriptional response by HSBP1. Genes Dev **12:** 1962-1974

Sayeed SK, Shah V, Chaubey S, Singh M, Alampalli SV, Tatu US (2014) Identification of heat shock factor binding protein in *Plasmodium falciparum*. Malar J **13:** 118

Searle BC (2010) Scaffold: a bioinformatic tool for validating MS/MS-based proteomic studies. Proteomics **10:** 1265-1269

Shen Z, Liu YC, Bibeau JP, Lemoi KP, Tuzel E, Vidali L (2015) The kinesin-like proteins, KAC1/2, regulate actin dynamics underlying chloroplast light-avoidance in *Physcomitrella patens*. J Integr Plant Biol **57:** 106-119

Shimada T, Koumoto Y, Hara-Nishimura I (2014) Evaluation of defective endosomal trafficking to the vacuole by monitoring seed storage proteins in *Arabidopsis thaliana*. Methods Mol Biol **1209:** 131-142

Shimada T, Yamada K, Kataoka M, Nakaune S, Koumoto Y, Kuroyanagi M, Tabata S, Kato T, Shinozaki K, Seki M, Kobayashi M, Kondo M, Nishimura M, Hara-Nishimura I (2003) Vacuolar processing enzymes are essential for proper processing of seed storage proteins in *Arabidopsis thaliana*. J Biol Chem **278:** 32292-32299

Suetsugu N, Sato Y, Tsuboi H, Kasahara M, Imaizumi T, Kagawa T, Hiwatashi Y, Hasebe M, Wada M (2012) The KAC family of kinesin-like proteins is essential for the association of chloroplasts with the plasma membrane in land plants. Plant Cell Physiol **53:** 1854-1865

Suetsugu N, Wada M (2007) Chloroplast photorelocation movement mediated by phototropin family proteins in green plants. Biol Chem **388:** 927-935

Sun Y, MacRae TH (2005) Small heat shock proteins: molecular structure and chaperone function. Cell Mol Life Sci **62:** 2460-2476

Tagaya M, Arasaki K, Inoue H, Kimura H (2014) Moonlighting functions of the NRZ (mammalian Dsl1) complex. Front Cell Dev Biol **2**

Tai LJ, McFall SM, Huang K, Demeler B, Fox SG, Brubaker K, Radhakrishnan I, Morimoto RI (2002) Structure-function analysis of the heat shock factor-binding protein reveals a protein composed solely of a highly conserved and dynamic coiled-coil trimerization domain. J Biol Chem **277:** 735-745

Truebestein L, Leonard TA (2016) Coiled-coils: The long and short of it. Bioessays **38:** 903-916

von Koskull-Doring P, Scharf KD, Nover L (2007) The diversity of plant heat stress transcription factors. Trends Plant Sci **12:** 452-457

Wada M (2016) Chloroplast and nuclear photorelocation movements. Proc Jpn Acad Ser B Phys Biol Sci **92:** 387-411

Wada M, Kong SG (2011) Analysis of chloroplast movement and relocation in Arabidopsis. Methods Mol Biol **774:** 87-102

Wang Q, Tu X, Zhang J, Chen X, Rao L (2013) Heat stress-induced BBX18 negatively regulates the thermotolerance in Arabidopsis. Mol Biol Rep **40:** 2679-2688

Weber C, Nover L, Fauth M (2008) Plant stress granules and mRNA processing bodies are distinct from heat stress granules. Plant J **56:** 517-530

Wellmer F, Riechmann JL (2010) Gene networks controlling the initiation of flower development. Trends Genet **26:** 519-527

Woehlke G, Schliwa M (2000) Walking on two heads: the many talents of kinesin. Nat Rev Mol Cell Biol **1:** 50-58

Yeh CH, Kaplinsky NJ, Hu C, Charng YY (2012) Some like it hot, some like it warm: phenotyping to explore thermotolerance diversity. Plant Sci **195:** 10-23

Yoo SD, Cho YH, Sheen J (2007) Arabidopsis mesophyll protoplasts: a versatile cell system for transient gene expression analysis. Nat Protoc **2:** 1565-1572

Zhao P, Liu F, Zhang B, Liu X, Wang B, Gong J, Yu G, Ma M, Lu Y, Sun J, Wang Z, Jia P, Liu H (2013) MAIGO2 is involved in abscisic acid-mediated response to abiotic stresses and Golgi-to-ER retrograde transport. Physiol Plant **148:** 246-260

Zhao P, Lu J (2014) MAIGO2 is involved in gibberellic acid, sugar, and heat shock responses during germination and seedling development in Arabidopsis. Acta Physiol Planta **36:** 315-321